LIGHT CURVE CHARACTERSTICS OF GAMMA-RAY BURST

By

Temam Beyan Tuki

A THESIS SUBMITTED TO

GRADUATE PROGRAMS OF
ADDIS ABABA UNIVERSITY

IN PARTIAL FULFILLMENT FOR THE REQUIREMENTS
OF THE DEGREE

MASTER OF SCIENCE IN PHYSICS

(ASTRONOMY/ASTROPHYSICS)

ADDIS ABABA, ETHIOPIA

OCTOBER 2022

ADDIS ABABA UNIVERSITY

PROGRAM OF GRADUATE STUDIES

LIGHT CURVE CHARACTERSTICS OF GAMMA-RAY BURST

By

Temam Beyan Tuki

Department of Physics

Addis Ababa University

Approved by the Examining Board:

Dr. Firaol Dirirsa _____ Signature
Advisor

_____ Signature
Examiner

_____ Signature
Examiner

Date: October 2022

ADDIS ABABA UNIVERSITY

Date: **October 2022**

Author: **Temam Beyan Tuki**

Title: **Light Curve Characterstics of Gamma-Ray Burst**

Department: **Department of Physics**

Degree: **M.Sc.** Convocation: **October** Year: **2022**

Permission is herewith granted to Addis Ababa University to circulate and to have copied for non-commercial purposes, at its discretion, the above title upon the request of individuals or institutions.

Signature of Author

This Work is Dedicated

to

My brothers Mulugeta Asfie and Kalamlak Azanaw died

in 1995/1997E.C

Table of Contents

List of Tables

List of Figures

Acknowledgements

First of all, I thanks to God for His unlimited love, care, and undesirable help He has done to me throughout my life. I would like to express my deep gratitude to my advisor and instructor Dr. Remudin Reshid for his continuous guidance and great support. I would like to extend my thanks to my instructors and the department of physics of the Addis Ababa University and its staffs, I have learned many things from them like respecting teaching profession, punctuality, encouraging learners to have creative mind and so on. I would also like to acknowledge the financial support for my studies provided by the Addis Ababa Educational Bureau. Finally, I am very grateful thanks to my friends Murad Yimam, Debela Alemayehu, Jemal Regassa, Natnael and all my classmates I have received many comments and feed backs.

Addis Ababa University
Temam Beyan Tuki
April, 2021

Abbreviations

ASD	Amplitude Spectral Density
AXPs	Anomalous X-Ray Pulsars
EFE	Einstein Field Equation
BBH	Binary Black hole
BBN	Big Bang Nucleosynthesis
BHNS	Black hole Neutron Star
CBC	Compact Binary Coalescence
CMBR	Cosmic Microwave Background Radiation
CW	Continuous Wave
PN	Post Newtonian
GRBs	Gama-ray Bursts
GR	General Relativity
GW	Gravitational Wave
LIGO	Leser Interferometer Gravitational Wave Observatory
LISA	Leser Interferometer Space Astronomy
MBH	Massive Black hole
NR	Numerical Relativity
SEOBNR	Spin Effective One Body Numerical Relativity
IMRPhenom	In-spiral Merge Ringdown Phenomenological
PSDs	Power Spectral Density
SGRS	Soft Gama-ray Repeaters
SNR	Signal to Noise Ratio
GRB	Gamma-ay burst
XRT	x-ray telescope

Physical Constants

Speed of Light	C = 2.99792458$\times$ 10^8 ms^{-1}
Universal Gravitational Constant	G = 6.67$\times 10^{-11} Nm^2kg^{-2}$
Mega parsec	Mpc = 3.08568025$\times 10^{24}$ cm
Planck luminosity	L_0 = 10^{59}egr/s
Mass of the Sun	$M_\odot$ = 1.99 $\times$ 10^{33} g
Kilo parsec	kpc = 3.08568025$\times 10^{21}$ cm
luminosity of the Sun	$L_\odot$ = 3.839 $\times 10^{33}$erg/s
Positive Cosmological constant	$\Lambda = (10^{16} ly)^{-2}$
Hobble's constant	H_0 = 70.65km/s/Mpc

Symbols

f_{GW}	Gravitational Wave frequency in Hz
L	Total radiated luminosity in erg/s
τ	Time remaining before coalescence in second(s)
M_c	Chirp mass in $M_\odot$
ρ_{crit}	Critical energy density in eV/cm^3
D_l	Luminosity distance of the from the source to Earth in Mpc
S_{GW}	Power spectral density in unit of egr/sHz

Abstract

We present new observations of the early X-ray afterglows of the first 27 gamma-ray bursts (GRBs) detected with the Swift X-ray Telescope (XRT). The early X-ray afterglows show a canonical behavior, where the light curve broadly consists of three distinct power law segments: (i) an initial very steep decay ($\propto t^{-\alpha}$ with $3 \lesssim \alpha_1 \lesssim 5$) , followed by (ii) a very shallow decay ($0.2 \lesssim \alpha_2 \lesssim 0.8$) , and finally (iii) a some what steeper decay ($1 \lesssim \alpha_3 \lesssim$1.5). These power law segments are separated by two corresponding break times, 300 s $\lesssim t_{break,1} \lesssim$ 500 s and 10^3 s $\lesssim t_{break,2}$t $\lesssim 10^4$ s.

On top of this canonical behavior of the early X-ray light curve, many events have superimposed X-ray flares, which are most likely caused by internal shocks due to long lasting sporadic activity of the central engine, up to several hours after the GRB. We find that the initial steep decay is consistent with it being the tail of the prompt emission, from photons that are radiated at large angles relative to our line of sight.

The first break in the light curve ($t_{break,1}$) takes place when the forward shock emission becomes dominant, with the intermediate shallow flux decay (α_2) likely caused by the continuous energy injection into the external shock. When this energy injection stops, a second break is then observed in the light curve ($t_{break,2}$). This energy injection increases the energy of the afterglow shock by at least a factor of f > 4 , and augments the already severe requirements for the efficiency of the prompt gamma-ray emission. Subject headings: gamma rays: bursts — radiation mechanisms: non thermal

CHAPTER 1

Physics of gamma-ray bursts.

1.1 Introduction

what are gamma-ray bursts?

Gamma-Ray Bursts (GRBs) are the most powerful explosions in the Universe and, arguably, represent the most significant new astrophysical phenomenon since the discovery of quasars and pulsars or the Big Bang. As their name suggests, GRBs are detected as brief, intense and totally unpredictable flashes of high-energy gamma rays, thought to be happened during the core collapse of super massive stars (long-soft bursts, T_{90} > 2 seconds) or the merger of two compact objects such as binary neutron stars or a neutron star and a stellar mass black hole (short-hard bursts, T_{90} < 2 seconds).[1]

They are the fastest extended objects of Nature, that injecting large amount of energy of order 10^{54} ergs or 10^{47} joules from very small compact region in a few seconds at cosmological distance. During explosion ,the energy they released for a few second to hundred seconds comparable to the energy that the Sun will emit in its entire 10 G years of life time. The overall observed fluence ranges from 10^{-4} ergs/cm^2 to 10^{-7} ergs/ cm^2 corresponds to the isotropic equivalent luminosity of 10^{48} to 10^{54} erg s^{-1} (fig 1.2) [1, 2].

Gamma Ray Bursts (GRBs) are at the intersection of many different areas of astrophysics: they are relativistic events connected with the end stages of massive stars; they reveal properties of their surrounding medium and of their host galaxies; they emit radiation from gamma-rays to radio wavelengths, as well as possibly non-electromagnetic signals, such as neutrinos, cosmic rays and gravitational waves. Due to their enormous luminosity, they can be detected even if they occur at vast distances, and are therefore also of great interest for cosmology [2].

During explosions, ultra relativistic jets are produced accompanied by an intense gamma-ray flashes called prompt emissions that outshine all the sky at very high red shifts.These prompt emissions are often followed by afterglow signals across the electromagnetic spectrum from X-ray to radio wavelengths covering timescales from tenth of seconds up to several months or more. [2, 3]

GRB events are classified as being either long (lasting > 2 s) or short (lasting < 2 s), separated by the length of duration $T_{90} \sim 2$sec, and spectral hardness of their prompt emissions, with long GRBs (LGRBs) believed to be associated with the deaths of collapsed massive stars, whilst short GRBs (SGRBs) more likely to be the result of either the merger of binary neutron stars (BNS) or the merger of a neutron star with a black hole (NS-BH) [3].

Due to their huge radiated energies, GRBs can be observed up to $z \sim 10$, therefore they are very powerful cosmological tools, complementary to other probes such as SN-Ia , clusters etc.The correlation between spectral peak photon energy Ep,i and intensity (Eiso, Liso, Lp,iso) is one of the most robust and intriguing properties of GRBs and a promising tool for measuring cosmological parameters [2, 3].

1.2 Historical Discovery of gamma-Ray bursts

Gamma-ray bursts (GRBs) were first discovered unexpectedly during the Cold War in the late of 1960_s by the Vela military satellites that were equipped with detectors of gamma-rays, X-rays and neutrons and launched by USA Air Force in collaboration with the Los Alamos National Laboratory.The first event was recorded in 1967.After verification, it was clear that gamma radiation was not of human origin, nor even terrestrial. However,the existence of Gamma-ray flashes coming from cosmos was announced the first event after six years in 1973 dating back to july 2,1967. [4]

The study of GRBs physics mainly led by observations with help of improved detecting instruments on satellites to monitor phenomena in the universe in relation to Gamma- ray emissions. Prompted by the instrumental progress from time to time, the story of observational research of GRBs from early time to recent classified in five eras . [4, 5]

1.2.1 Dark era (1967-1990)

The first gamma -ray burst discovered named as " GRB 670702" that detected by vela satellite (see fig 1.1).In the name " GRB 670702", the first two digits represent the burst year, the middle two and the last two digits represent month and the last two digits date of the burst. If more than two events of bursts were happened in one day, they labeled to identify them using English letters alphabetically .[5]

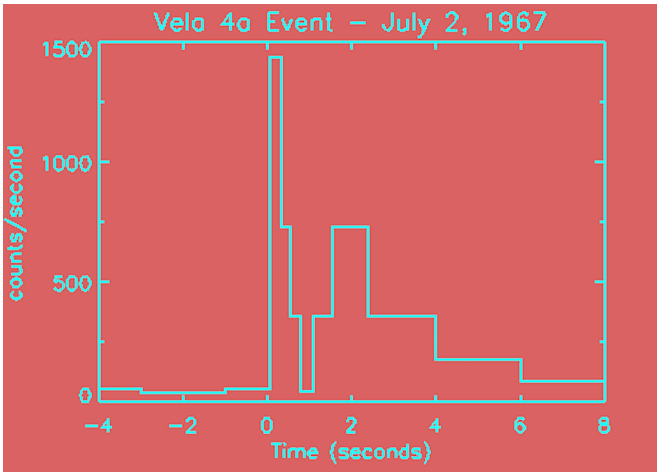

Figure 1.1: Light curve of the first gamma -ray burst (GRB670702) detected by Vela. Two separate pulses can be identified over a duration of less than 10 seconds. [4]

After the first discovery , the series of vela satellites were launched , and more than 70 GRBs were detected. These earliest observational result of GRBs only consists several structures “spikes” were found in Gamma-ray band , but no way to identify their location due to lack of improved instrumentations . However, after series of vela satellites were launched with improved detecting instruments , the origins of GRBs believed to be out side the solar system by offset information [4, 5].

The three fundamental questions raised during the era were :
Where are GRBs come from ? What are the source of such flashes of light? By what mechanisms do they appear in our Milky way galaxy ? or in more distant galaxies ? To answer such burning questions at the time , more than a hundred models were proposed to explain the origin and production mechanisms of GRBs. However , only a few of models were able to explain that GRBs events occurred at cosmological (

far distances). On the other hand , the majority of the models were indicating that the events of GRBs closer to the Earth (galactic origin) apparently to overcome the energy out put. During the dark era , the detection and interpretation of GRBs were stagnent due to lack of improved detecting instruments , however GRBs as new field of science was opened at the end of the era .[4, 6]

1.2.2 BATSE era (1991-2000)

The Burst And Transient Source Experiment (BATSE) was the early advanced space detecting instruments that carried on the Compton Gamma-Ray Observatory (CGRO) , that capable to map Gamma-ray sources from almost the entire sky in energy range of (20keV - 2MeV). Between 1991 and 2000 , BATSE detected 2704 GRBs , as shown in the diagram below. It can be seen that they are fairly uniformly spread over the entire sky , indicating that they are either nearby and clustered around our position , or they do not originate in our Galaxy. The contributions of BATSE in its nine years successful operations were:

• At its early operation in 1991 , the apparent isotropic spatial distributions of 2704 GRBs were confirmed (see fig 1.2) , and then the cosmological origin of GRBs was accepted by astronomers although the debate between galactic and cosmological origin of GRBs continued until BeppoSAX. [5] [7]

The fig below shows that the distribution is « isotropic »: the bursts are distributed randomly on the map indicating that they are either very close to the Earth , or very far , of extra galactic origin. No concentration of bursts along the plane of the Milky Way , symbolized on the map by the horizontal center line , appears. This most likely excludes candidates from our galaxy.

Long duration , bright bursts are shown in red , while shorter , weak bursts appear in purple. The bursts in grey are those for which the fluence could not be calculated , because of incomplete data. (The fluence indicates the total energy passing through a unit area ; in X-ray astronomy , the unit of fluence is erg cm-2.)
•Fireball model as the theoritical tool to explain the huge amount of energy drived from observed flux and fast time variability.
• confirm the classification GRBs into two types (short and long GRBs) according

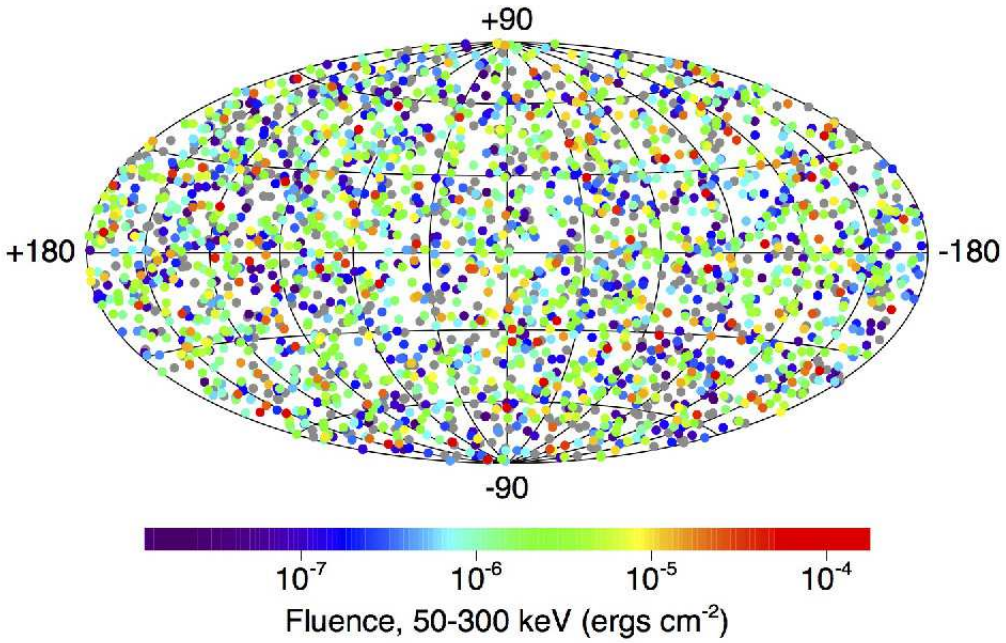

Figure 1.2: The distribution of all 2704 GRBs detected by BATSE satellite: they are clearly isotropic distribution .[7]

to bimodal distribution of duration parameter T_{90}.

•provide database of GRBs, their spectral and temporal properties [7].

limitations of BATSE

• unable to classify diversities GRBs light curves (single spikey pulses , smooth with or multiple peaks , very erratic , chaotic and spiky).

• BATSE's observations remain limited to gamma - rays alone , no other follow-up at other longer wavelengths. [6, 7]

1.2.3 Bepposax era (1997-2000)

Bepposax equipped with improved instruments on satellite launched in 1997. It was designed to detect long -living afterglows from X-ray to radio wavelength. In 1997 , BeppoSAX detected the first X-ray afterglow within a GRB error box (GRB 970228). An optical transient was also found, fading within a week (HST press release). The identification of GRB 970228 with a host galaxy at a known distance (red shift of 0.695) confirmed the cosmological origin of GRBs.The contributions

of BATSE in its seven years operations were:

• confirm the precise location of the burst in the X-rays rapidly transmitted and also discovered weak and decreasing signals.This was the late-time , weaker emission radiates in the X-rays , optical and radio waves.
• Opened a new era for the current understanding mysteries of GRBs.
• predicted the existence of GRBs afterglow in longer energy bands (from optical to radio wave length).
•Provide clues for GRB-SN possible connection , which was latter confirmed by HETE-2 and Swift that support collapser model and explosions of massive star of wolf-Rayet (WR), leaving behind BH.
•Provide crucial information on the progenitors of GRBs.
•X-ray flash as new class of GRB with less-lumineous and low redshift identified from traditional GRBs.[4, 7]

limitation of Beppo-sax
• unable to show the canonical behavior of x-ray afterglow which was later revealed by swift .[5]

1.2.4 Swift era (2004-now)

Swift was a robotic space satellite that launched on November 20, 2004 and become fully operational in 2005. It has been designed for multi-wavelength approach to detect X-ray, optical and radio bands: called afterglow emissions . Swift has unique capability of performing fast autonomous slews to track the GRB and its afterglow with minimum delay. Swift aimed to investigate four phenomena : progenitors of GRBs , different physical processes underlying different classes of GRB observations , the interaction between blast wave and its surroundings and early evolution of Universe via GRBs. Furthermore, swift aimed to investigate non- electromagnetic waves (GRBs) related phenomenae such as neutrions , cosmic ray and gravitatinal waves . In its ten years operations , Swift detected more than 2300 GRBs. [4, 6]

The swift's three instruments on-board - the Burst Alert Telescope (BAT), X-ray Telescope (XRT) and Ultraviolet and Optical Telescope (UOVT) -that working together and they enabled to study the prompt and afterglow emissions over a broad range of wavelengths. (see fig 1.3) The three swift instruments and their functions described below:[8][9]

Burst Alert Telescope (BAT).

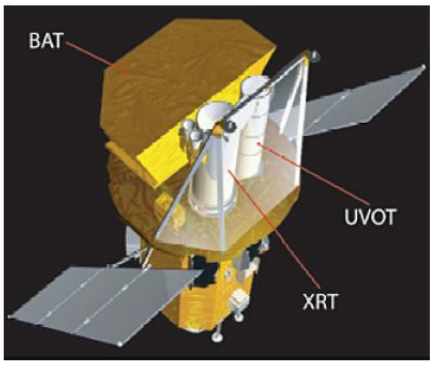

Figure 1.3: Schematic view of the swift satellite(Gehrels et.al 2004).The size of Mask of BAT is $2.7m^2$ [7]

BAT detects GRB event and computes its coordinate (position) in the sky and locates the position of each event with an accuracy of 1 - 4 arcminutes with in 15 seconds. This position immediately relayed to the ground and rapid slew-ground based telescope catches the informations.

X-Ray Telscope (XRT)

It takes image and perform spectral analysis of the GRB afterglow. It provides more precise position of GRB with a typical error circle of approximation 2 arc seconds radius. The XRT also used to perform long term monitoring of GRB afterglow light curves and operated in energy range of 0.2 keV - 10 keV .

Ultra Violet optical Telescope (UVOT)

UVOT used to detect optical afterglow and provide a sub-arc seconds position. It also used to provide longer wave length follow ups of GRB afterglow light curves. Swift has been a great success in its observations.

• Revealed unusual behavior “canonical" X-ray afterglow and X-ray flaring activity during the afterglow phase.

• provides the capability to obseve the transition from prompt to afterglow emissions and detect the high-z GRBs such as 050904,080913 and 090423,which were the most distant cosmic explosions [5] [7].

1.2.5 Fermi era (2008-now)

Fermi designed to focus on prompt emissions phase of GRBs by using much higher energy ranges (8keV - 300keV) than swift (15keV -150keV).It carries on board two types of detectors known to be Gamma-Ray Burst Monitor (GRBM) and Large Area Telescope (LAT).They provide unprecedented spectral coverage for seven orders of magnitudes of energy from 8 keV to 300 GeV.Fermi made Significant progresses for the current understanding of origin of GRBs.
The contributions of Fermi since launched were:
• The existence of three elemental spectral components (Band function-like, thermal and extra non-thermal power-law component) in GRB spectra was confirmed.
• Suggest that the featureless Band function spectra extended from keV to Gev band a Poynting-flux-dominated flow.
• Explain the existence of thermal components in some GRBs(e.g GRB 5090902B) due to hot fireball without strong magnetization.
• The delayed onset of GeV emission in some LAT GRBs suggests that there likely be a change of either particle acceleration condition or the opacity of the fireball during the early prompt emission epoch.
• confirms that long lived GeV emission is likely of external origin, while GeV emission during the prompt phase, on the other hand is likely of internal origin [10] [11].

1.3 Classification of gamma-ray bursts

Based on the bimodal distributions of duration T_{90} or T_{50} of prompt phase or hardness ratio , GRBs have been catagorized in to two groups: short/hard and long/soft GRBs. The duration of GRB,T_{90} or T_{50} , is defined by the time interval over which 90 % or 50 % of the burst fluence is detected respectively. The typical duration of a GRBs is $\sim$ 20 - 30 seconds for long bursts and $\sim$ 0.2 - 1.3 seconds for short one. Observational result tells us that the duration of GRBs can be in a range of 5 orders of magnitude, i.e, from $\sim 10^{-2}$ s to $\sim 10^{3}$ s. The bimodal distribution of T_{90} has been used to identify the two categories of GRBs, namely, “long” or "soft" (T_{90} $\geqslant$ 2 s) and “short” or " hard "($T_{90} \leqslant$ 2 s) (see Fig1.4). Instrumentally , T_{90} or T_{50} depends on the energy band and the sensitivity limit of the detector. Theoretically, there are three timescales which may be related to the observed GRB duration T_{90}:
(1) central engine activity time scale t_{eng}
(2) relativistic jet launching time scale t_{jet}

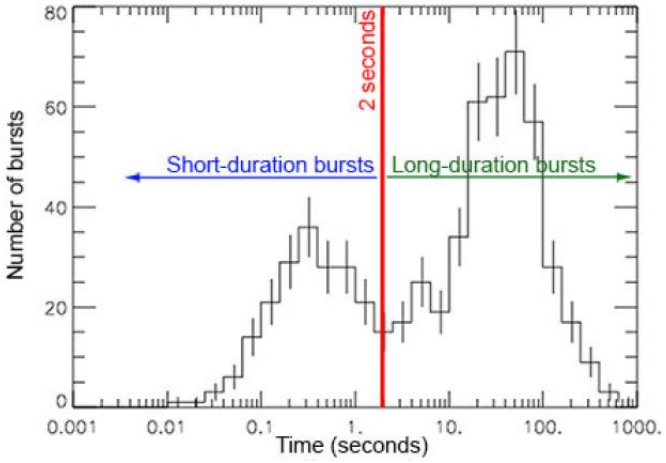

Figure 1.4: The GRB classification (long and short) distributions. They last between a few milliseconds and several minutes. The two populations 'short' and 'long' with duration peaking around 0.3 seconds and last aound 30 seconds , with the 'divding line' between them being $\sim$ 2 seconds. [9]

(3) energy dissipation time scale t_{dis} . Then, the observed GRBs with duration T_{90} should satisfy: [5]

$$T_{90} \leq \delta t_{dis} \leq \delta t_{jet} \leq \delta t_{eng} \tag{1.1}$$

1.3.1 short/hard gamma-ray bursts

Short / Hard gamma ray bursts (SGRBs) are events with a duration T_{90} less than 2 seconds and account for about 30% of the total gamma ray bursts. such out bursts are so strong that they produce ripples in the fabric of space-time called gravitational waves. Short GRBs were likely caused when two ultradense stellar corpses known as neutron stars collided and formed a black hole , or when a black hole ate a neutron star. They are highly energetic / hard gamma-rays when compared with their long burst counter parts. For many years short-hard GRBs were not deeply researched as long GRBs. As a result, the study of short-hard GRBs (SHBs) limited. However, one year after swift launch, in 2005 a breakthrough occurred following the first detections of SHB afterglows. [5] [6]

The swift observations established that SHBs are cosmological relativistic sources that, unlike long GRBs, do not originate from the collapse of massive stars, and therefore constitute a distinct physical phenomenon. One viable model for SHB origin is the coalescence of compact binary systems , in which case SHBs are the electromagnetic counterparts of strong gravitational-wave sources. In this burst, the conversion of energy into gamma- rays decreases as the burst progresses. There

is no radio, optical, or x-ray counterpart has found for any short burst [5].

1.3.2 long/soft gamma-ray bursts

Another sub class of GRBs that account for 70% and have a duration of greater than 2 seconds are classified as long/soft GRBs (see fig 1.4 above). All long bursts display x-ray afterglow and about one-half as radio or optical afterglows. In long duration bursts energy conversion appears to remain constant through burst. Their creation linked to a young galaxies with rapid star formation and to a core collapse of powerful supernova (hypenova) occurred when massive stars collapsed to black hole.This is unambigeously associating long GRB with the death of massive stars at high red shift originated in star -forming regions. Hypernovas are 100 times brighter than typical supernovas and are thought to be generated by stars that are spinning particularly fast or have an especially strong magnetic field, imparting extra energy to their combustions.[6]

1.3.3 Ultra long gamma-ray bursts (ULGRBs)

GRBs with highly a typical duration of more than 10,000 sec called ultra-long gamma-ray bursts (ulGRBs).They are the tail end of the standard long GRBs that caused by the collapse of a blue supergiant star,tidal disturption events or a new born magnatar. They have been proposed to form a new third class of GRBs. One explanation which has been proposed for their ultra-long duration is that they could have progenitors differ from classical GRBs in that: they could be produced either by the core collapse of a low-metallicity supergiant blue star, the birth of a magnetar following the collapse of a massive star or the collapse of a Pop III star.In any case, it is clear that the duration of these bursts make them so peculiar that they need further study [10][11].

1.4 Gilobal properties of GRBs

Two distinct global properties of “classical GRBs” began to emerge—the intensity /brightness and the angular / location distributions—both are important implications for the distance scale of GRBs and hence their origin.

1.4.1 Intensity distribution

The brightness distribution of GRBs appeared to show that we were seeing out to the edge of the GRB population:there were too few faint GRBs relative to the

number expected if GRBs were uniformly (“homogeneously”) distributed in space. Brightness was most straight forwardly measured as the peak flux (F , with units [erg s^{-1} cm^{-2}]) in the light curve of a GRB. The brightness distribution is usually measured as the number, N(>F), of GRBs brighter than some peak flux F per year. If the peak luminosity (L, with units [erg s^{-1}]) of all GRBs is the same, then, using the $\frac{1}{r^2}$ law, for a given flux F we would see all the GRBs within a maximum distance:[7] [12]

$$d_{max} \approx \sqrt{\frac{L}{4\pi F}} \propto F^{\frac{-1}{2}}$$

All the GRBs to that distance would be brighter than F by construction. The number of GRBs we would detect to that brightness (or brighter) in one year would just be the volume times the intrinsic rate (R, in units of [event yr^{-1} per volume element]):$N(>F) \propto V \times R \propto R \times d_{max} \propto R \times F^{\frac{-3}{2}}$. So with a homogeneous distribution, we expect that the number of faint GRBs N should grow as a power law proportional to $F^{\frac{-3}{2}}$, where the constant of proportionality scales directly related to the intrinsic rate R: for every ten times fainter in flux we observe, we would nominally expect about thirty-two times more GRBs. While this was indeed seen for the brightest events,there was a flattening at the faint end of the brightness distribution. This flattening was highly suggestive that we were seeing the “edge” of the GRB distribution in space,an important clue in understanding the distance scale. But without knowing the intrinsic luminosity L, we could only infer the shape of the distribution, not the scale. It was like seeing a picture of a building but not knowing if it was of a miniature in a snow globe or the life-sized version .[7] [12]

1.4.2 Angular distribution

The locations of GRBs on the sky appeared to be randomly (isotropically) distributed: that is, there was no indication that any one direction on the sky was especially more apt to produce GRBs than any other (see fig1.2 in section 1.1).If GRBs were due to neutron stars strewn through out the disk of the Galaxy, for instance, the locations of GRBs on the sky should have been preferentially located near the Galactic plane (as is seen with SGRs). If associated with older stars in the roughly spherical “bulge” of the Milky Way, GRBs would have been preferentially located in the direction toward the Galactic center and less so toward the opposite direction.

The inference that the Sun was roughly at the center of the GRB distribution in space,while casting aside some models, still allowed for a variety of distance scales: from a fraction of a light year to billions of light years [7].

1.5 Statement of the problems

As mentioned in section 1.1 above ,to study the mystery and phenomenology of Gamma-ray bursts , several satellites (from Vela at early time to Fermi and others at recent time) equipped with different instruments (telescopes) have been launched. Among those satellites , swift was open new era for the current understanding and development of gamma ray researches.Swift missions detected prompt and afterglow emission phases of gamma-ray burst. Not only this, the temporal and spectral behaviors ,Light curve properties of x-ray and optical afterglow of gamma-ray burst also studied in detailed. However, as far as my search /review literature is concerned, there is knowledge gaps explaining more about canonical x-ray afterglow light curves:

• Does x-ray afterglow results of internal or external shocks of fireball?

• What parameters / variables responsible for the variations of temporal and spectral indices of canonical x-ray afterglow ?

• what are the features and implications of these indices ?

• Did all afterglow x-rays in agreement with canonical behavior ?

In this thesis, I emphasized on the theoretical and observational properties of canonical X-ray afterglow light curves qualitatively and quantitatively.

Regarding this work unclear ideas or un answered questions are listed below. Among these:

(1) what are the cause of canonical x-ray light curve of afterglow gamma-ray bursts?

(2) what are the progenitors of canonical x-ray light curves?

(3) Did the value of temporal index of any random x-ray afterglow confirmed to the proposed value in all phases of canonical x-ray ?

(4) Could some of the breaks at end of the plateau phase actually be jet break or late steep decay phase? The goal of this thesis is attempt to explain and give answers for these questions.

1.6 Objectives of the thesis and its outline

General objective

The main objectives of this thesis is to study the light curves as well as temporal and spectral properties of canonical behavior of x-ray afterglows. and the temporal and spectral features.

specific objectives

•To explain the cause and effect for the variations of light curves of prompt and afterglow phases.

•To compare / contrast the calculated values of temporal and spectral indices of x-ray afterglow with the proposed one .

•To describe the features and implications of temporal (α) and spectral (β) indices of x-ray afterglows.

Thesis outline

Hereafter, I point out the outline of the thesis. In chapter 1 above, the background of gamma -ray bursts , the historical discoveries of gamma -ray bursts, , gradual development of gamma -ray burst in (pre -swift era : from 1967 up to 1997) and after swift era , their classification would be discussed. In chapter 2 , I intended to explain the emission mechanisms of both phases of GRBs as well as their theoretical and observational properties using standard fireball models. Furthermore , I discussed about the canonical behavior of x-ray afterglow and its flux decaying with time deeply.

In chapter 3, I addressed the method and methodology , models and tools used to analyze the collected data for some selected short and long gamma-ray bursts with the known redshifts. In chapter 4, I discussed on achieved results / findings and comparing /contrasting with proposed values using tables and figures . Finally, I put a brief summary or review of the enlightenment of this work , and forward suggestion on unexplored area of the field for future research in the last chapter.

CHAPTER 2

Emission mechanisms and observational properties of gamma-ray bursts

2.1 Introduction

This chapter comprises eight sections that logically related to explain gamma -ray physics. Overall , the phenomenology of gamma - ray bursts : emission mechanisms of gamma-ray bursts, observational properties of gamma-ray bursts (prompt and afterglow phases), interpretation of gamma-ray afterglow especially x-ray afterglow , decaying of flux with time are discussed subsequently. Finally flux (F) and light curve intensity (f) are defined and their equations are derived briefly.

2.2 GRBs production mechanisms

GRB emission mechanisms:- are the theories or models that visualize or explain how the energy from GRBs progenitor (sources) is turned to radiation. In the early 1990's more than 100 potential models were developed to describe the phenomenon of GRBs. However, more constraining observations over the years have resulted in the development of a standard model called " Fireball model " to describe well about the emission mechanisms of GRBs and their afterglow , properties of GRBs progenitors. It was a neat theoretical standard model that has been revised that attempt to explain the mysterious events of GRBs for a longer time.[13]

2.2.1 Basic fireball model

Gamma-Ray Bursts (GRBs) are the most energetic events in the universe. During GRBs, the most powerful energy equal to over 9000 supernovae can impressively ejected. These energy levels are so extreme that they cannot be created by thermal processes. So, what causes these high energy levels? The Fireball Model is one of the few models that has been put f orth to explain why GRBs tend to have such

high energy levels. It also attempts to explain the time scales that govern the phenomenology of prompt and afterglow phases.[13] [14]

The variability of GRBs light curves directly related to the high energy levels , as the variability indicates that it occurs over a very small area with the emission of GRB energy being in the order of 10^{52} ergs , coming from a very small volume of space with highly concentration of radiation energy, and then theorized that a Lorentz factor of Γ $\sim$100 be associated with the GRB.In short, the fireball model must be able to encompass all of these variables in order to apply to all GRBs (and thus be a plausible model to study GRB physics.[14]

The name of the fireball model suggests the mechanism to which a GRB occurs in a fireball of ultra-relativistic energy consisting of optically thin material with very few baryons. In essence, during the GRB event, the inner engine remains undetectable due to the optical thickness and the lack of a thermal profile due to the compactness problem .The highly relativistic expansion of fireball overcome the compactness problem and can cause the internal shocks that produce the detectable GRB, while the external shocks form the gradual afterglow [15].

The first relativistic fireball model was proposed by (Paczynske 1986,Goodman 1086).They had shown that the sudden release of a large quantity of gamma ray photons into a compact region can lead to an opaque photon–lepton “fireball” through the production of electron–positron pairs $e^{-}e^{+}$. The most fundamental property the fireball can be characterized by its initial energy E_o. In the fireball there are M_o baryons (electrons have negligble mass) with $M_o \ll \frac{E_o}{c^2}$, and its mean energy per baryon, $\eta = \frac{E_o}{M_o c^2}$ [14, 15].

Fireball model predicted that when the expanding plasma becomes optically thin , and hence the emitted radiation escapes within created burst . This mechanism would generate a quasi-thermal spectrum rather than the observed power-law spectra, thus indicating the difficulty inherent to explaining the duration of the GRB having such a small timescale (just a few seconds). Moreover, the fireball baryonic load is another model which converts all its energy into kinetic energy rather than into luminosity to produce a quasi-thermal spectrum. This model, however, does not explain the efficient emissions of radiation. In particular, the origin of the emission associated with the two phases is produced by two different

mechanisms: a matter-dominated, and a radiation-dominated. The assumption that the fireball is matter-dominated is widely used, and which consists of baryons , electrons and positrons , and photons resulting from the merger of binary neutron stars or a collapse of massive stars .[10] [15][16]

The emitted energy is higher than the mass of the baryon in the rest frame by

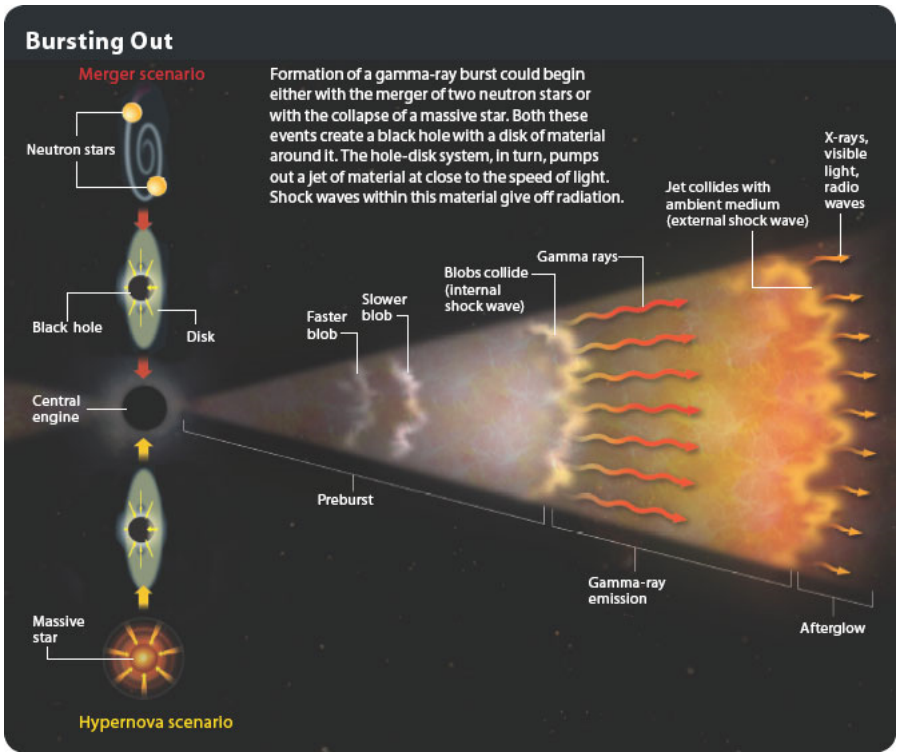

Figure 2.1: Visualization of the fireball model that illustrates the various steps of basic standard model with the internal and external shocks and radiations. At the left the two main scenarios (collapser and merger) indicated that they lead to a central black hole surrounded by a disk. (from Gehrels et al. (2002), credit Juan Velasco)[13]

a factor of $\sim$ 100, with the baryon accelerated with in an expanding fireball to a higher Lorentz factor, Γ. During this process, two major out comes can be seen: at the photosphere, a fraction of the thermal energy is radiated away and the accelerated electrons produce a non-thermal gamma ray spectrum by a synchrotron or an IC processes in the internal shock at large jet radius. Rather, the outflows that formed from the central engine are believed to be dominated by Poynting flux.[15][16]

The shocks in the fireball model are collisionless, whereby the particles involved are accelerated and scattered within the Fermi process when crossing the shock

interaction. This can result in the type of energy distribution that can be described by a power law ($\alpha \sim$ 2 - 3). In such a situation, the electrons emit a non-thermal radiation of photons via two different mechanisms, synchrotron and Inverse compton scattering, that extend to very high energy (GeV bands).[16] [17].

Disspative process

Disspative process :- is the of outflows or shock waves from central engine interact with interstellar medium (ISM) to produce both GRBs and its afterglow - the external and internal shock models, that successfully interpret the prompt and afterglow emissions respectively.In particular, the origin of the emissions associated with the two phases is produced by two different processes. [8] [17].

Internal shock model

Internal shock model : is the model that highly obseved energetic gamma -rays flash produced and explained by fireball model. Immediately after the initial GRB event, shock waves emanate from the inner engine at relativistic speed (99.995% of the speed of light) and a Lorentz factor of ~ 100. The fireball is dynamic object that contains a mixture of charged particles , photons , and magnetic fields known as plasma , in which the particles move fast with random motions . In the context of early evolution of a GRB , the fire ball carries the energy deposited near the central engine and expands outwards radially. During expansion several shock waves are emanating from the compact source , and are traveling at different relativistic speeds . Thus , the interaction between different shock wave fronts cause energetic gamma-ray emissions. [17][18]

The internal shocks traveling at relativistic speeds convert kinetic energy into gamma-ray photons, this is the only way to get high energy gamma-rays that are observed (as previously mentioned, they cannot be emitted through a thermal process). When internal shocks interact with each other as they are moving at relativistic speeds, the interactions produce Inverse Compton and Synchrotron emissions.fig 2.2 [18] Initially, the fireball is optically thick but as it expands and cools down and becomes optically thin, allowing the gamma-ray photons to escape. Early models had the fireball and the internal shock waves as being purely radiative, but this didn't follow what was being observed (it would have made a profile too smooth). To solve this problem, some baryonic mass was added. This allowed for the internal shocks to become effectively contaminated. The added baryonic mass

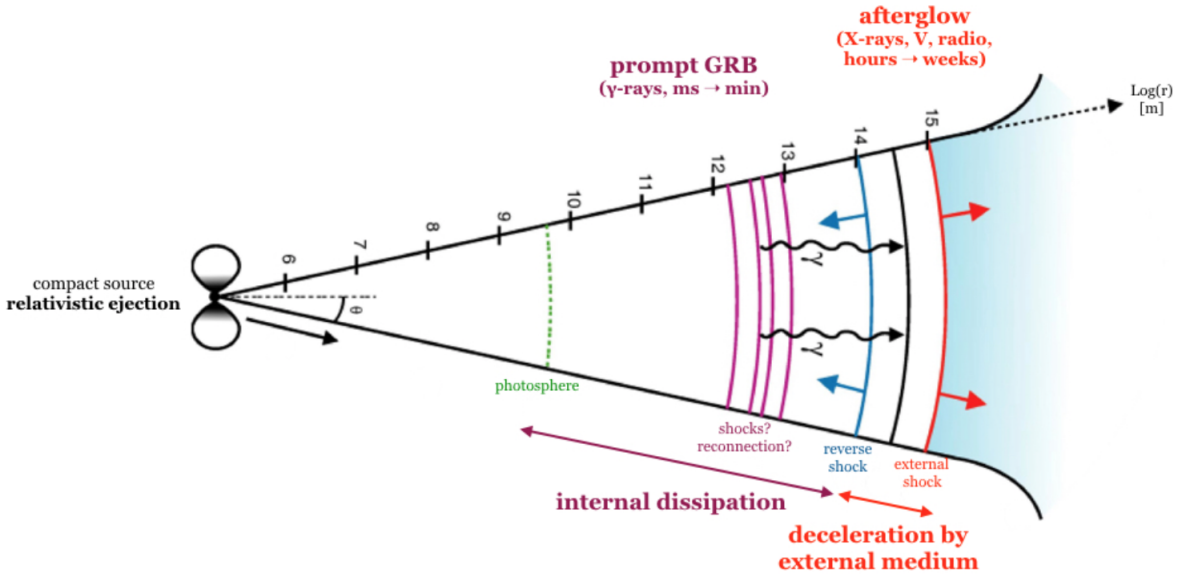

Figure 2.2: Standard fireball model.

also aids in the conversion of some radiation energy into kinetic energy, which helps with an added kick to the relativistic kinetic energy of the shock waves, this in turn increases the gamma-ray energy more,Even if all of the shock waves emanate from the core at the same speed they will eventually cross over multiple times. As the shells are emitting through inverse Compton, it is slowing the shock front, thus increasing the times that many shock waves interact with one another. The earlier shock waves are likely to be emitted slower than the later shock waves, this would also increase the amount of interactivity between the different shock waves.[16][18].

External shock model

The external shock waves are used to explain the afterglow that was first detected by BeppoSAX in 1997, as the internal shock waves are not able to explain the duration of the afterglow nor the wavelengths that are detected (which range from soft x-ray through to radio). The name can be a little misleading at first; the external waves actually refer to the internal waves at a later stage –once they've cooled down and continue emanating from the source. As the shock waves continue out they will eventually interact with the Interstellar Medium [ISM] (such as a molecular cloud or some other impedance), and it is the shock waves' interaction with the dust/gas that cause the afterglow . Unlike the internal shocks, the external shocks are primarily a thermal emission(see fig 2.3). The energy transferred from

the shock waves is deposited into the ISM; this material can then be caught up in the shock front and emit radiation. As the shock waves began with a lot of energy, there is a lot that can be deposited into the ISM, this is what can cause such long afterglow and why it covers all parts of the energy spectrum .[19][20]. A relativistic

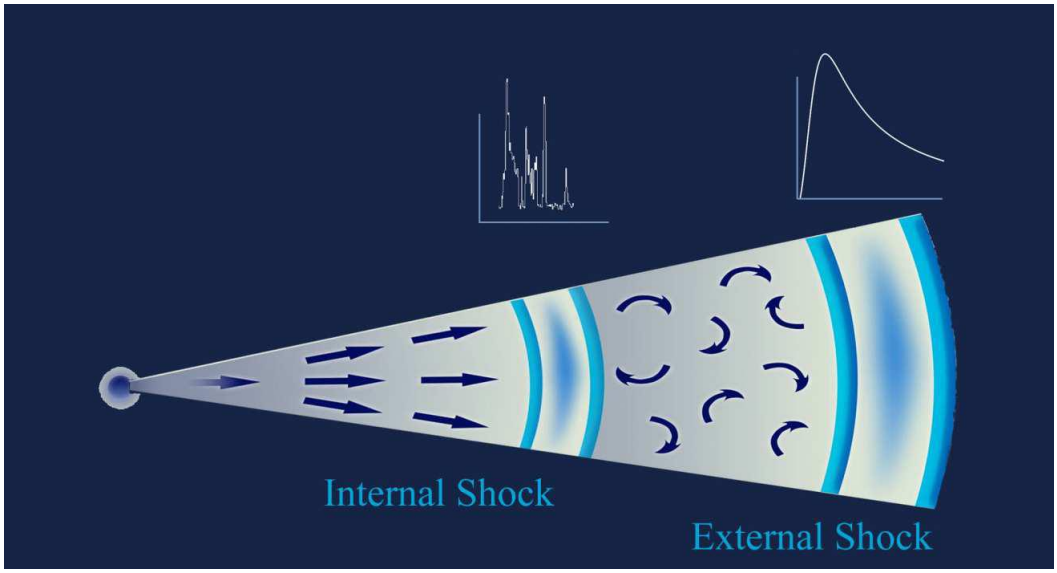

Figure 2.3: schematic view of the structure of the relativistic jet produced by the gamma-ray burst. The external shock arises as a result of the impact of the jet on the stellar wind of the progenitor. This is where the final goodbye of the SOS similar emission from the collapsing star forms, which is characterized by a smooth (but non-monotonic) light variation. The internal shock persists as long as the central engine continues operating this is where rapidly varying gamma-ray , x-ray and optical radiation formed.[21]

materials/jets are running into external ambient medium or stellar wind. In each time, the ejecta run a high density environment in which they produced a peak in the mission called external shock . In the external shocks, the jets may be forward shocked or reverse shocked.As the material in the jet expands, accelerates and compresses interstellar medium,It creates a forward shocks. The deceleration of forward shocks is occurred when the rest mass energy of the swept up particles equal to the ejected energy. This sets a deceleration length scale at ($\sim 10^{16}$ cm) . The reverse shock is formed by the deceleration of the jet material and propagates back into the relativistic flow. This happens when the rest mass energy of the swept up particles is greater than the ejected energy .[20]

Although it would be correct to assume that all GRBs have an external shock, about half of detected GRBs don't have a detectable afterglow. The reason that no

afterglow being detected is not thought to be the exposures aren't long enough, or because we're observing too early or too late. Rather, GRBs occur in high mass systems, whether it be through a supernova or NS-NS and NS-BH merges, this means that they had very short stellar lives and may still be inside of a molecular cloud. Molecular clouds are very optically thick environments so the reason we're not able to detect the afterglow in about 50% of the time could just be due to reddening, absorption, or scattering.[20, 21]

Radiative process

Synchrotron Radiation

Synchrotron emission is the non-thermal radiation produced when a relativistic electron gyrates in a uniform magnetic field. Synchrotron radiation can explain the GRB prompt emissions, and is considered to be one of the more important mechanisms in various astrophysical phenomena. synchrotron shock mechanism, which is produced by the optically thin plasma in a weak magnetic field, can be used to predict the form of the observed spectra [1][15] [18]

Synchrotron emission can be classified as having two regimes: the "fast-cooling" phase,which describes when the timescale for the cooling of the electrons is shorter than the dynamical lifetime of the source, resulting in an electron that cools quickly compared to the low-level injection of energy; conversely, "slow-cooling" occurs when the timescale for the cooling of the electrons is longer than the dynamical lifetime of the source . The differences between these two regimes are associated with the emission's radiative timescale [9] [10].

The peak frequency, the cooling frequency, and the self-absorption frequencies set the characteristic break frequencies in the synchrotron spectra. These frequencies evolve with time;indeed, their evolution is reflected in the complexities observed in the shapes of the light curves at certain band energies . This model can successfully describe the afterglow. Thus, the optically thin synchrotron spectrum is currently considered the best spectral fitting model for most GRBs. The first synchrotron model was applied to the spectral fitting of GRBs by Tavani (1996), and subsequently by Baring and Braby (2004)[15][22]

Synchrotron Self-Compton

Inelastic collisions between low-energy photons and ultra-relativistic electrons are

known as the IC processes. Each astrophysical source has an Synchrotron Self-Compton (SSC) scattering component when synchrotron radiation that energizes it provides the means to scatter its seed photons to high energies and across a large frequency range. Thus, the phenomenon responsible for creating high-energy emissions from GRBs and other astrophysical sources is accepted to be the SSC mechanism. The SSC mechanism, while complex, uses a simple power-law function to explain the injected electron spectrum. The SSC spectrum can be described precisely as carrying out a complicated seed photon spectrum convolution and electron energy distribution. In certain circumstances, the GRB spectrum can be modelled as an SSC component at very high energy $\sim$10 MeV.[11][16]

2.2.2 GRBs progenitors models

There are three models to produce lots of energy in nature: nuclear, gravitational, and rotational. The nuclear energy does not have enough efficiency to power a GRB. For example, the proton-proton chain that is responsible for energy production in stars has an efficiency of about 0.0067 which was not enough to power a GRB. However , the last two mechanisms (gravitational and rotational) are playing greate roles powering GRB energy release. The central engine that produces the initial energy, E_o , is hidden from direct observation. However, the observed temporal structure is thought to reflect the activity of the central engine.[23]
The central engine must satisfy the following general features:
• Capable of producing an extremely relativistic energy flow containing $\approx 10^{51}$ - 10^{55} erg.
• Highly variable flow resulting in highly variable light curves.
• Its activity can last from a fraction of a second to a few hours.
• Possibility of late time activity that may cause X-ray flares.
• Relatively rare event as suggested by observed GRB rates.

2.2.3 Working mechanisms of central engine

The central engine is of great importance, as it needs to be able to push material out very near the speed of light. The inner engine of a GRB is a highly compact source, and it is the highly compact nature of this object that leads to the idea that the core of the inner engine of a GRB is either a neutron star or a black hole (as they're the two most compact sources that we're currently aware of) The workings of this inner engine will alter depending on whether it is a long or short GRB being observed.

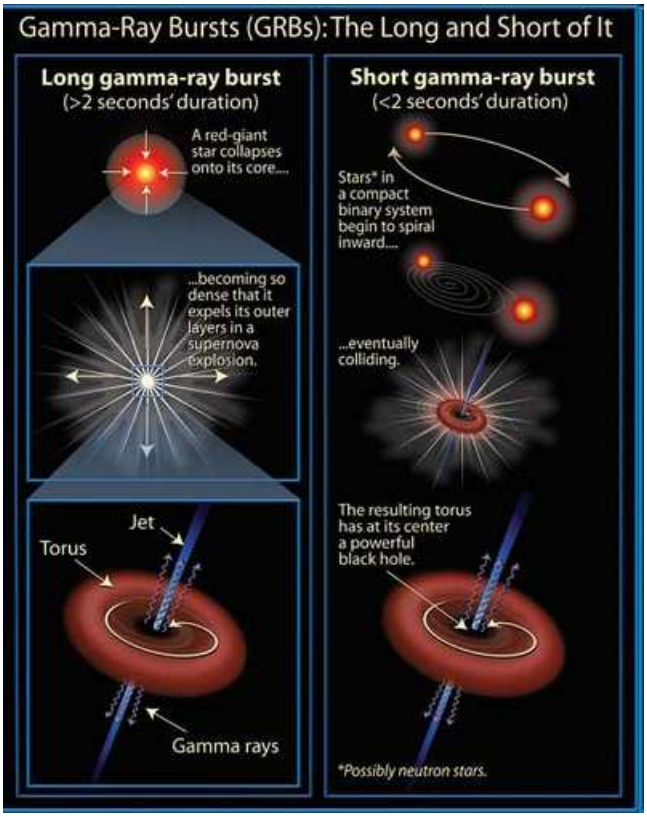

Figure 2.4: Schematic scenarios for plausible progenitors of long and short GRB. Long GRBs come from the collapse of massive , while rapidly rotating stars and short GRBs result from the merger of compact objects.[23]

A short GRB has been thought as occurring during a neutron star binary collision [NS-NS] or a neutron star-black hole collision [NS-BH]. It has been suggested that a long GRB could be associated with a hypernova when a Wolf-Rayet type star undergoing a core collapse supernova.[21][23]

2.2.4 Supernova

Supernovae (SNe) are highly powerful explosions that terminate the life of some stars. The study of SNe was initiated in early 1930s by W. Baade and F. Zwicky , and the first bright supernova (SN 1987A) was reported in 1987. It was suggested that , the source of enormous quantity of energy released in SNe is the gravitational collapse of a star to neutron star. During explosion , some solar masses are ejected in the interstellar space with a kinetic energy of the order 10^{51} erg. The ejecta contains heavy elements that are vital for the chemical evolution of galaxies, stars, and planets. SNe may be sources of cosmic rays , and Some compact remnants such as a neutron star or a black hole.[24]

According to observational properties , supernovae explosions are classified as Type I and Type II. where the former and the latter characterized by absence and presence of hydrogen lines in the spectrum respectively. Each type has its own characteristic light curve, although a wide variety of deviations from the general shape is detected, resulting from individual properties Type I supernova arises

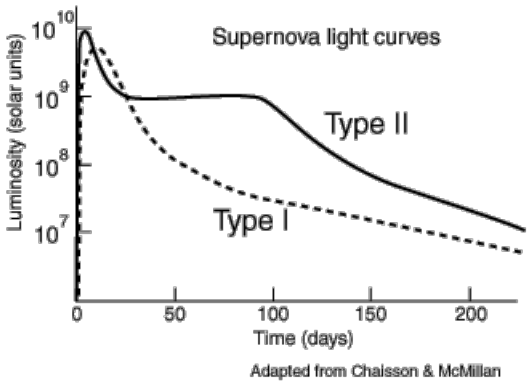

Figure 2.5: Supernova light curves

When white dwarfs are collapsed and reaching the Chandrasekhar limiting mass by accertion where as Type II supernovae that are associated with the collapse of iron cores of massive stars. These stars have large hydrogen rich envelopes; hence the evidence of hydrogen in the spectrum. If a supernova's spectrum contains lines of hydrogen it is classified Type II; otherwise it is Type I. As massive stars evolve much more rapidly than low mass stars, old stellar populations, where no star formation occurs, have outgrown the Type II supernova stage (see fig 2.5 above). [24][25]

According to the observed features at early spectral explosion , Type I SNe further classified in Type Ia, Ib and Ic. Type Ia supernovae are characterized by the presence of a clear (Si II) absorption line around 6150 Å and their late spectra show many lines associated with Fe emission , while Type Ib and Ic supernovae do not show this ionized silicon (Si II) absorption line and are distinguished according to the presence or not, respectively, of moderately strong He I lines around 5876 Å.[26]

Type II SNe can also be sub-divided based on their spectra. and they show very broad emission lines which indicate expansion velocities of many thousands of kilometers per second have relatively narrow features in their spectra. These are

called Type IIn, where the 'n' stands for 'narrow'. They can potentially be produced by various types of core collapse in different progenitor stars, possibly even by type Ia white dwarf ignitions , although it seems that most will be from iron core collapse in luminous super giants or hyper giants. The narrow spectral lines for which they are named occur because the supernova is expanding into a small dense cloud of circumstellar material.[27]

The other sub division supernova is "Type IIb" that used to describe the combination of features normally associated with Types II and Ib. These supernovae , like those of Type II , are massive stars that undergo core collapse. However the stars which become Types Ib and Ic supernovae have lost most of their outer (hydrogen) envelopes due to strong stellar winds or else from interaction with a companion .[26][27]

2.2.5 GRB-SN associtation

The early 1980s flashes or bursts of γ - ray light were detected with space probes from diverse directions in the sky. It then also became known that the earlier US military satellites Vela (1967- 1984) , designed to detect the γ - ray flash from atomic bomb explosions , had seen such bursts. With the Burst and Transient Source Experiment (BATSE), on board of the Compton Gamma Ray Observatory (CGRO), launched in 1991, many more such flashes were detected.[27]

In the late 90s it was realized that, in addition to the normal core collapse and thermonuclear explosions, there are more energetic supernovae with an energy output and 10^{45} J, i.e., they are at least 10 times as energetic as a normal supernova that is 5 - 50×10^{44} J. These are now often referred to as hypernovae (HNe) or alternatively as broad lined supernovae, since they have very broad lines. SN 1998bw was also observed as an LGRB (long gamma ray burst), establishing the first connection between a GRB and a supernova, the death of a massive star. [25][27]

In addition, many GRB afterglows show bumps in the light curve that are consistent with an underlying hypernova like event. Interestingly, at present all GRB supernovae are classified as SNe Ic, i.e., supernovae that have lost both their hydrogen and their helium envelopes . Hypernovae are produced by more than one type of event: relativistic jets during formation of a black hole from fallback of material onto the

neutron star core, the collapsar model,or during the last phases of the coalescence of neutron star binaries. These catastrophic events are believed to exist at the central engine of highly energetic gamma-ray bursts [28]

Stars with initial masses between about 25 and 90 times the solar mass of the sun develop cores large enough to create a black hole after a neutron star formed by supernova explosion and some material will fall back onto it. In many cases this reduces the luminosity of supernova, and above 90 $M_{\odot}$ the star collapses directly into a black hole without a supernova explosion. However, if the progenitor is spinning quickly enough the in falling material generates relativistic jets that emit more energy than the original explosion.

In some cases these can produce gamma ray bursts, although not all gamma ray bursts are from supernovae. Some black hole binaries appear to be linked to the hypernovae believed to power gamma - ray bursts . In our GRB the materials are fallback but not a collapsar because the amount of falling mass is small and it don't have to be collapse in to Black Hole.[29]

2.3 Observational properties of gamma-ray bursts

GRBs composed of two main radiative phases: the prompt and afterglow phases.The former typically observed in soft gamma-ray (10 keV to 10 MeV), and generally lasts between $\sim$ 100ms and $\sim$ 1000 s, although there is a wide variety of different temporal behaviors observed,from single pulses to complex temporal evolution. The spectrum of this prompt emission is non -thermal, often described by a Band function with a typical peak around $\sim$ 200 keV. The afterglow emission is most often detected from X-rays to radio waves and fades away with time. In the optical, the temporal fading goes typically as t^{-1} , however the slope of this fading depends on the wavelength and on the burst. This means an afterglow observed in the optical will frequently fade beyond the reach of most ground - based telescopes within a week. In the radio however, there is evidence of emission from the afterglow up to a few months or even years after the burst. Sudden flash of gamma rays emitted in the creation of a GRB was the route by which GRBs were detected and the property for which they are named. The prompt emission is readily detected, even by rudimentary space-based gamma - ray detectors, due to the extreme high-energy photon budget that GRBs exhibit.Indeed, at peak, GRBs outshine all other

sources within gamma-ray sky, including the Sun.[18]

2.3.1 Prompt emission of gamma - ray bursts

prompt emission of GRBs is defined as the emission observed during gamma-/hard X-rays phase, whose photons are triggering the space instrumentation leading to multi-wavelength follow-up observations. It is believed to be the direct outflow ejected from the central engine; as per the "fireball" model , deposits its gravitational energy into a thermal explosion. In other words, the prompt emission occurs when the kinetic energy from a catastrophic explosion event, such as massive star core collapse or the merger of two compact stars, is converted into electromagnetic radiation due to the internal shocks that result from collisions between shells of ejecta.[23]

prompt emission generated due to internal shocks magnetic dissipation within the fireball take place effectively above the pair production (photosphere at 10^{12} to 10^{14} cm).These shocks splits from mini-shells within a jet produced by unsteady accretion of materials onto black hole or by the merger of binary neutron stars (BNS). The shells have a distribution in lorentz factor $\gamma \propto \Gamma$ where Γ is bulk lorentz factor.[22][23]

Ground-based facilities have detected radiation up to a trillion times the energy

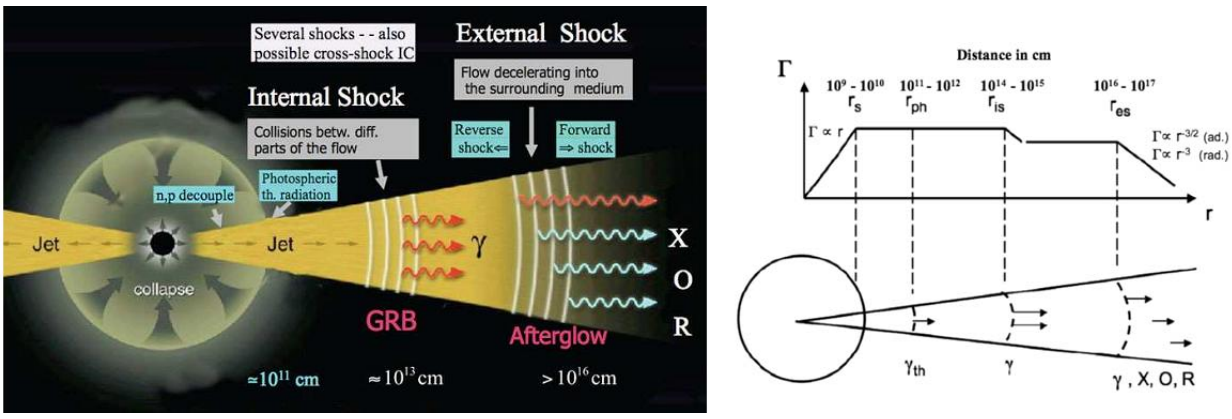

(a) **(b)**

Figure 2.6: (a) Collapser model shows internal and external shocks producing prompt and afterglow emissions respectively.
(b) Schematic evolution of the jet Lorentz factor and examples of symbolic locations of radii : the saturation radius r_s , photospheric radius r_{ph} , internal shock radius r_{is} and external shock radius r_{es}

of visible light from a cosmic explosion called a gamma-ray burst (GRB). This illustration shows the set-up for the most common type. The core of a massive star (left) has collapsed and formed a black hole. This “engine” drives a jet of particles that moves through the collapsing star and out into space at nearly the speed of light. The prompt emission, which typically lasts a minute or less, may arise from the jet’s interaction with gas near the newborn black hole and from collisions between shells of fast-moving gas within the jet (internal shock waves). The afterglow emission occurs as the leading edge of jet sweeps up its surroundings (creating an external shock wave) and emits radiation across the spectrum for some time — months to years, in the case of radio and visible light, and many hours at the highest gamma-ray energies yet observed. These far exceed 100 billion electron volts (GeV) for two recent GRBs. Credit: NASA’s Goddard Space Flight Center

In the region around $\sim 10^{12}$ cm to 10^{14} cm , the collisions between different parts of the flow is produced in different shells (see fig 2.6 (a) and(b)). As a fast shell catch up with a slower ones, they form strong internal shocks that propagates in both shells with out deceleration. Once shell became above the photo sphere,the heated and accelerated electrons cool by synchrotron emission then radiation is observed in γ-ray band. Each collision that occurs above pair photo sphere produces a pulse in the GRB’s light curves [22]

Thus, GRB light curves represent the count rates/photons recorded by the high energy detectors as a function of time. Each of the recorded events shows different variability patterns, meaning that each light curve is different from the rest. As shown in Figure 2.7 , the light curves can be classified into four different categories Pe’er, 2015:

- Single-peak events (e.g. GRB 910711)
- A smoothed light curve composed with several peaks (e.g. GRB 920221)
- Separated multi-collisions (e.g. GRB 930131A) and
- Irregular peaks (e.g. GRB 991216)

The result is that the fireball expands due to the effects of thermal pressure and is then accelerated to relativistic speeds, where the thermal energy is ultimately released in the form of photons at the photo sphere. In the internal shock case, the dissipation happens inside the ejecta, where the ejecta is decelerated by the surrounding medium and this deceleration happens after the internal shock phase ceased. [6][23]

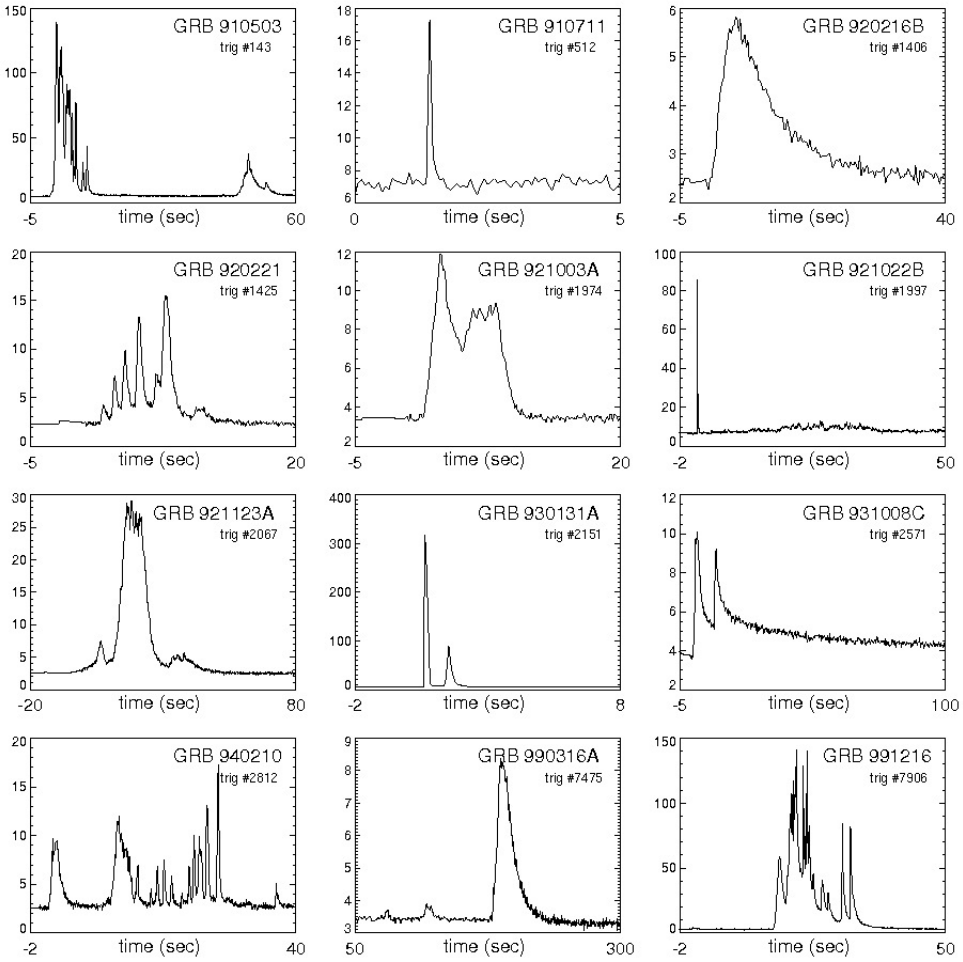

Figure 2.7: Diverse light curves of the GRBs prompt emission detected by BATSE instrument.This sample includes short and long events.

[Firaol Fana]

2.3.2 Afterglow emission of gamma - ray bursts

Afterglow gamma - ray burst studied extensively since the launch of swift.Afterglow emission is created by the collision between ejected bursts and the surrounding medium or interstellar gas or dust , and fading slowly at longer wavelength. The GRB itself is rapid, lasting from less than a second up to a few minute at most. Once it disappears, it leaves behind a counterpart at a longer wavelengths from X-ray to radio bands . Then, they are remain detectable for day or longer. As we have mentioned above, afterglow emissions are dominated by external shocks. Due to luck of advanced instrument, early searches were unsuccessful largely to observe the bursts' position at a longer wavelength immediately after the initial burst,Once the GRB faded deep imaging was able to identify a faint, distance host of galaxy at a location of GRB as pinpointed by the optical afterglow.[15][22][23]

2.4 Interpretations of afterglow gamma- ray bursts

Before launch of the Swift satellite, broad-band, late time (t > $\sim$ 10 hours) afterglow data had been collected for a moderate sample of GRBs. These observations were generally consistent with predictions of the external forward shock,synchrotron emission, model. The main observational properties of late time afterglow radiations are:

• In general the optical afterglow displays a power law decay behavior $F_\nu \propto t^{-\alpha}$, with a decay index $\alpha \sim 1$. This is consistent with the prediction of the standard external shock afterglow model.

• A temporal break in the optical afterglow light curve is usually detected for bright GRBs. The break time is typically around a day or so, which is followed by a steeper decay with slope $\alpha \sim 2$. This is consistent with the theoretical prediction of a "jet break".

• The radio afterglow light curve initially rises and reaches a peak around 10 days, after which it starts to decline (e.g. Frail et al., 2000). The peak usually corresponds to passage of the synchrotron injection frequency ν_m , or the synchrotron self-absorption frequency ν_a , through the radio band.

• The broad-band afterglow spectrum can be fit with a broken power law, at a fixed observer time as one expects for the synchrotron afterglow model.

• For bursts with high-quality data richer features in the optical light curves have been discovered, which include bumps and wiggles that deviate from the simple afterglow model predictions. Smooth bumps in afterglow light curves with duration $\delta t_{obs} \sim t_{obs}$ may be interpreted as due to density bumps in the external medium where as sharper features in light curves might be due to energy injection from the central engine angular fluctuations in energy per unit solid angle [18].

2.4.1 Early time afterglow

2.4.2 Late time afterglows

Before swift mission, afterglow observations was started after several hours (10 hrs) after bursts trigger. The optical afterglow of late time displays a power law decay behavior $F_\nu \propto t^{-\alpha}$, with a decay index $\alpha \sim 1$. The temporal break in optical afterglow light curve was detected for bright GRBs. The break time is typically around a day and followed by steeper decay with decay slope of $\alpha \sim 2$. The radio

afterglow light curve initially rises and reaches a peak around 10 days after starts to decline . The peak usually corresponds to the passage of synchrotron injection frequency ν_m or synchrotron self absorption frequency $\nu_a$through the radio band. The broad band afterglow spectrum can be fit with a broken power law at a fixed observer time. [24][25]

2.5 Theoritical interpretation of X-ray afterglow

One of the breakthrough discoveries by Swift was the X-ray afterglow behavior in the first few hours after a GRB, which were missed by Beppo-SAX. Swift revealed several striking features of x-rays : (i) many early X-ray light curves show a canonical behavior with three distinct power-law segments (marked I - III in Fig 2.8 right), in some cases also a jet break at later times (IV); (ii) in about half of the GRBs, bright flares in the X-ray light curves are observed long after the end of the prompt phase (10^2 s - 10^4 s). In some extreme cases, these flares have integrated energy similar to, or exceeding, the initial burst of gamma rays, and severely challenge current theoretical models.[26]

Afterglow gamma-ray bursts observed at all wavelengths such as: X-ray , optical , IR, and radio . X-ray afterglow is the first and strongest, but shortest signal.In fact it seems to begin already while the GRB is going on. X-ray light curve observed several hours after the burst can usually be extrapolated to the late parts of the prompt emission. Due to its low variability and observed time range (from minutes to weeks after the GRB event), a canonical X-ray light-curve for the afterglow was defined from the result of Swift /BAT-XRT instruments.[27][28]

The four segments, with their corresponding temporal indices , are associated two by two and identified as early and late afterglows . segments I and II are the steep and s hallow decay respectively , while segments III and IV respectively a standard afterglow and a jet break . Part I and III, marked by solid lines, are most common and the other two components, marked by dashed lines , are only observed in a fraction of all bursts. Part I, thought to be associated with the prompt phase when the central engine is still active; the rest of the afterglows are due to the dynamics of the interaction between the jet and the surrounding medium. [30][31] [32]

GRBs early afterglows detected within less than 100 seconds after trigger in the

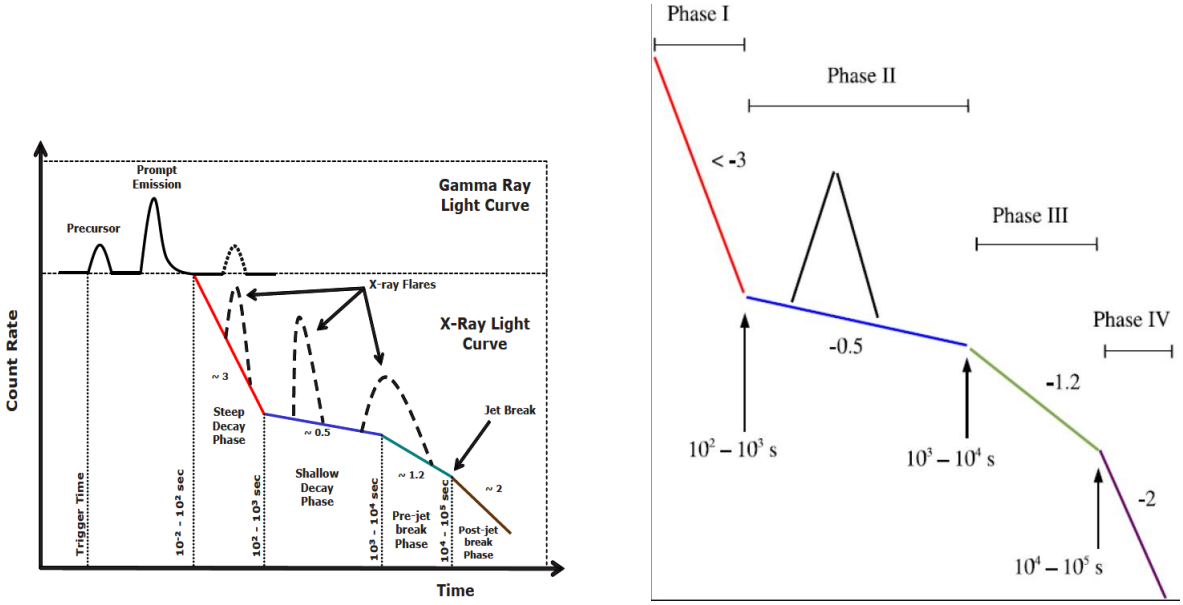

Figure 2.8: (a) Canonical GRB light curve , showing prompt phase followed by afterglow phase.
(b) Canonical x-ray light curves with its components: a steep decay phase (typical index of 3) which can then break to a shallower decline (shallow decay phase), a standard afterglow phase (pre-jet break phase), and possibly, a jet break and post-jet break phase. Sometimes an X-ray flare is seen.

swift mission. The canonical X-ray afterglow light curve generally includes four phases such as early time steep decay phase, the shallow decay /plateau phase, normal decay phase and late steep decay phase [33].

2.5.1 Early steep decay afterglow x-ray light curves

. This phase is the tail of prompt emission that governed by curvature effect, for which emission from different viewing angles reaches the observer with different delays due to the light propagation effects [33]. The relationship between temporal and spectral slopes of higher latitude emission is $\alpha = 2 + \beta$. It is independent of any of the environmental or other parameters such as peak frequency and cooling frequency that affects the closure relations for the external shocks. [34]
Swift answer the debate of separation between prompt emission and late afterglow regarding to internal and external origin of the prompt emission i.e internal shocks are the origin of prompt emission.[33] [34] As shown in (Fig2.8 above), slope of early steep decay is around $3 < \alpha_1 < 5$. This phase may be simply the high

latitude emission associated with the prompt gamma-ray sources at $R \gtrsim 10^{15}$ cm when the central engine turns off faster than the decline of the X-ray light curves . On the other hand, if the emission region is at much smaller radius than the rapidly declining X-ray light curve reflects the time dependence of central engine activity.[35][36]
Detailed analysis of a sample of GRBs suggests that the high latitude "curvature effect" model can explain the early steep decay phase [37]. As we have shown in (Fig 2.8), the achromatic change of phases for sample GRBs indicates the light curves transition. These GRBs followed the decay power law relation $F_\nu \propto t^{-\alpha_1}$ where, $\alpha_1 = 2 + \beta$ for curvature effect model. Generally, this phase has already stayed between the time interval of $10^{-2} - 10^2$ seconds and $10^2 - 10^3$ seconds that presented (in fig 2.8) at the right side.

2.5.2 Shallow /plateau decay X-ray light curves

The shallow phase sometimes called plateau phase and characterized by very small decay with value of decay $0.5 < \alpha_2 < 1.0$. It rises when the energy ejected to the decelerated external shock. When the energy is terminated, the decay of light curves become slow down and the transition to phase III (normal decay) is occurred . In this phase, the shape of light curves in the X-ray and optical bands should be similar where breaks occur at the same time in these bands.[38][39]

Behind shallow / plateau phase there are two acceptable explanations: (1) There is a smooth and gradual energy injection arrives in the forward shock , due to the decrease of the Lorentz factor Γ at the end of prompt emission. The mass injected to the forward shock is the function of its lorentz factor and the energy injected. As a result Γ increases monotonically with radius where as the flux decays as a power law and depends on the mass and the energy injected .[40] [41]
(2) The central engine of the source stays active for hours after the burst and injects the smooth and continues energy at later times, several times after the burst. X-ray plateau resulted from the contribution of prompt X-ray emission scattered by dust in the host galaxy. [41].
[42].

2.5.3 normal decay of x-ray light curve

The normal decay is the III phase in the canonical x-ray afterglow. It has a decay slope around $1.0 < \alpha_3 < 1.5$ which was expected before swift and consistent with standard fireball afterglow model in ISM [56]. Its explanation is related to the end of energy injection at the external forward shocks. This situation happend when :
(1) The Lorentz factor is falling up to the point of minimal Lorentz factor that carries a significant initial energy in external for ward shock.
(2) The central engine needs to be inactive. In general the normal decay is expected in the standard forward shock.[43]

2.5.4 Late steep decay following the plateau in X-ray light curves

The IV phase represented at the left side of fig 2.8 with the decay slope greater than 2. After the normal decay, X-ray emission is powered by a continues jet from a long lasting central engine. Then X-ray flux from the external shock is buried beneath this emission [58]. Indeed, the canonical X-ray light curve can be matched with the accretion history in the collapsar GRB model. This model assume that the X-ray luminosity is proportional to the accretion power of the central engine [59]. This late steep decay of swift, represents an achromatic steepening that happens due to the jet breaks. When the Lorentz factor of the ejecta becomes larger than θ_0^{-1} compared to the jet opening angle θ_0 , the ejecta is collimated into a jet break. Finally, this phase is expected in the forward shock model as a jet break. Jet breaks are thought to happen due to the beaming of emission from GRBs. This phase has pre-jet-break phase and post-jet-break phase, (see in Fig 2.8).[44] [45]

2.5.5 Time breaks in swift X-ray afterglow

As shown in (Fig 2.8), there are three break points and the time at that points are called breaking time of afterglow light curves. These break times are the first break time, the second break time and the jet break time.

2.5.6 The first break in the light curve ($t_{break,1}$)

It is the time at which the phase of light curves changes from phase I to phase II is took places. As it has been shown in (Fig2.8), the $t_{break,1}$ is around $t_{break,1}(10^2 - 10^3)$ s < t_1 < $t_{break,2}(10^3 - 10^4)$ seconds).
The first break time is also the time when the slow decaying emission from the

forward shock become dominant over the rapidly decaying flux from the prompt emission at a large angle. In sharply decaying flux, the prompt emission initially dominates over the external shocks at t > $t_{break,1}$[**?**].

2.6 Flux decay with time of observed light curve

The fluence (S) is the total radiant energy collected from the GRBs per unit area over the duration of the event (i.e., T_{90}). It is computed by integrating its energy flux over time and the energy range of the detector (i.e., the total energy collected per unit time and per unit area). The fluence measured between energies E_{min} and E_{max} is given by[Firaol Fana]

$$S = T_{90} \int_{min}^{max} E \frac{dN}{dE} dE \tag{2.1}$$

The energy flux of a burst is defined

$$F = \int_{Emin}^{Emax} E \frac{dN}{dE} dE \tag{2.2}$$

When relativistic, conical and optically thin source moving with a Lorentz factor Γ turns off abruptly, the flux declines rapidly with time [47]. In such type of source which is specified with spherical co-ordinate (r, θ, φ), the source turned off at $r = R_0$. where r is the radius of the photo/jets, R_0 is the radius of the observer and θ is measured with respect to the line of sight to the observer. The time dependence

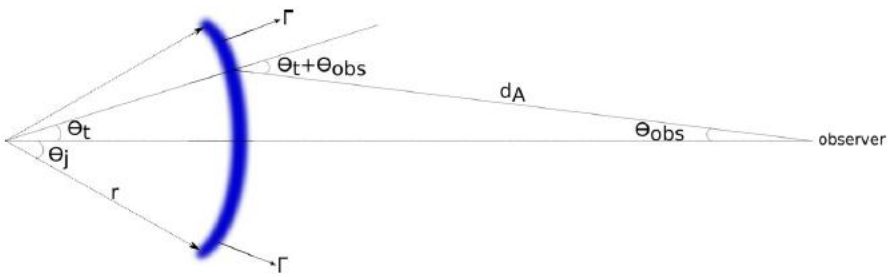

Figure 2.9: A sketch of the various angles and distances for the large angle (or high latitude) emission when the γ -ray source turns off suddenly.

of observed flux follows from the lorentz transformation of specific intensity. The specific flux in the observer frame from the relativistic source of moving object with specific intensity $I_{\nu'}$ and spectrum frequency $\propto \nu'_{-\beta}$ is given by

$$f_\nu(t_{obs}) = \int d\Omega_{obs} I_\nu cos\theta_{obs} \tag{2.3}$$

where $d\Omega_{obs}$ is the solid angle of the source, I_ν is the specific intensity of the source photon. To derive the standard flux decay of GRBs, let we define $d\Omega_{obs}$ and I_ν in the relativistic beaming.

In relativistic beam of photons, the transverse component of the momentum does not change under Lorentz transformation,i.e its comoving and lab frame values are the same. Thus

$$\nu sin\theta = \nu' sin\theta' \tag{2.4}$$

or

$$sin\theta = \frac{\nu'}{\nu} sin\theta' \tag{2.5}$$

Since the photon frequency on the observer frame, ν, can be expressed in terms of the comoving frequency, ν', using standard Lorentz transformation of photon as

$$\nu = \frac{\nu'}{\Gamma(1 - \frac{\upsilon cos\theta}{c})} = \nu' D \tag{2.6}$$

where D is standard Doppler effect which is expressed as $[\Gamma(1 - \frac{\upsilon cos\theta}{c})]^{-1}$. Then the ratio of the frequency become $\frac{\nu'}{\nu} = \frac{1}{D}$ and substituting this ratio into Eq. (2.5), we obtain

$$sin\theta = \frac{sin\theta'}{D} \tag{2.7}$$

For large Γ , $\theta \approx \frac{\theta'}{\Gamma}$. This tells us photons are focused in the forward direction such that the angular size of photo beam in the lab frame is smaller than it is in the comoving frame by a factor $\sim \Gamma$. And also the solid angle for a canonical beam of photons in lab frame is smaller than in the comoving frame by a factor of $\sim \Gamma^2$. This implies the Lorentz transformation of solid angle is:

$$d\Omega = sin\theta d\theta d\phi = \frac{sin\theta' d\theta' d\phi'}{D^2} = \frac{d\Omega'}{D^2} \tag{2.8}$$

The other parameter in the Lorentz transformation is the specific intensity. It is defined as flux per unit frequency and solid angle carried by photos traveling with in a narrow conical beam with its axis perpendicular to surface dA. This means

$$I_\nu = \frac{dE}{d\nu dt_{obs} dA d\Omega} \tag{2.9}$$

Considering $d\nu' dt' obs dA'$ = $d\nu dt_{obs} dA$, are Lorentz invariant and using Eq. (2.8) and $E = \Gamma E'$, Eq. (2.9) can be reduced to

$$I_\nu = D^3 I'_{\nu'} \tag{2.10}$$

Since for intrinsic spectrum, $I'_{\nu'} = I'\nu'^{-\beta}$,where β is spectral index, then the specific intensity is summarized as

$$I_\nu = D^3\nu'^{-\beta}I' \tag{2.11}$$

This equation, can be simplify by substituting the value of ν' from the Eq. (2.6)

$$I_\nu = D^{3+\beta}\nu^{-\beta}I' \tag{2.12}$$

Finally substituting Eq. (2.8) and Eq. (2.12) into Eq. (2.3) and integrating over $d\phi$ in the interval $0 - 2\pi$, the observed flux becomes,

$$f_\nu(t_{obs}) = 2\pi \int d\theta_{obs} \frac{I'_\nu \nu_0^\beta sin2\theta_{obs}[(1+z)\Gamma]^{-(3+\beta)}}{2\nu^\beta(1 - \upsilon cos(\theta + \theta_{obs})/c)^{3+\beta}} \tag{2.13}$$

where ν'_0 is the frequency that lies on the power law segment of the spectrum for $I'_{\nu'}$. Using the law of sine from the diagram in Fig. 2.8, we see that $sin\theta/dA = sin\theta_{obs}/R_0$, this implies $sin\theta_{obs} = \frac{R_0 sin\theta}{dA}$ and substituting into Eq. (2.13) ,in the case $\theta_{obs} \ll \theta$, yields

$$f_\nu(t_{obs}) = \frac{2\pi I'_0 \nu'_0 \nu^{-\beta}}{[(1+z)]^{3+\beta}}(R_0/dA)^2 \int_{\theta t}^{\pi/2} d\theta \frac{sin\theta cos\theta}{(1 - \upsilon cos\theta/c)^{3+\beta}} \tag{2.14}$$

Using substitution method of integrating, this equation can be simplified as

$$f_\nu(t_{obs}) \propto [(1 - \frac{\upsilon cos\theta_t}{c})]^{-(2+\beta)}\nu^{-\beta} \tag{2.15}$$

Photons released at ($r = \upsilon t$, θ, φ) arrive at the observer frame with a time delayed to a photon emitted at $r = 0$ of

$$t_{obs} = t - \frac{\upsilon \cos\theta}{c} = t(1 - \frac{\upsilon cos\theta}{c}) = t/\Gamma D \tag{2.16}$$

From this equation, the relation between t_{obs} and D is $t_{obs} \propto D^{-1}$. Then the flux decay with time of the observed light curves from Eq. (2.15) is summarized as:

$$f_\nu(t_{obs}) \propto t^{-(2+\beta)}\nu^{-\beta} \tag{2.17}$$

The standard convection of flux decay is

$$f_\nu(t_{obs}) \propto t^{-\alpha}\nu^{-\beta} \tag{2.18}$$

where $\alpha = 2 + \beta$

2.7 calculating luminosity (L) of x-ray afterglow

Luminosity is the total amount of electromagnetic energy radiated (out put) by an object per unit of time. The observed isotropic-equivalent luminosity in the X-ray afterglow ,L_x can generally be expressed as

$$L_x(t) = \int_{\nu_1}^{\nu_2} L_\nu(t) d\nu \tag{2.19}$$

where $L_\nu(t) = \frac{4\pi d_L^2 F}{(1+z)}$,substituting $L_\nu(t)$ in to equa. (2.4) reveals

$$L_x(t) = \frac{4\pi d_L^2}{(1+z)} \int_{\nu_1}^{\nu_2} \frac{F_\nu}{(1+z)[(1+z)t] d\nu} \tag{2.20}$$

where d_L is the luminosity distance, ν_1 and ν_2 are the spectral frequencies in the energy band, z is the red shift and $L_\nu(t)$ is the spectral luminosity at the cosmological frame of the source, i.e, both ν and t are measured in the frame [62].

$$L_x(t) = 4\pi d_L^2 \int_{\nu_1/(1+z)}^{\nu_2/(1+z)} F_\nu[(1+z)t] d\nu \tag{2.21}$$

since $F_\nu(t)$ is measured in the observer frame and assumed in standard form, Eq. (2.21) can be reduced to:

$$L_x(t) = 4\pi d_L^2 (1+z)^{(\beta-\alpha-1)} F_x(t) \tag{2.22}$$

where $F_x(t) = \int_{\nu_1}^{\nu_2} F_\nu(t)$. Here, we have understood that the flux decay of afterglow light curves are governed by standard power law of decay, i.e $f_\nu(t_{obs}) \propto t^{-\alpha}\nu^{-\beta}$,where $\alpha = 2 + \beta$. This is a theoretical understanding for the afterglow era. Therefore , swift observation have led to better understanding of afterglow x-ray light curves for the initial few hours. The two mechanism of emissions have related to the behavior of central engine of the burst. Now let us introduce the method and material used to analyze the temporal and spectral indices of canonical x-ray afterglow light curve in the next chapter.

CHAPTER 3

Research methodology

3.1 Introduction

The observational and theoretical understanding of prompt and afterglow phases of gamma-ray bursts suddenly changed after 20 , November 2004 , the launch of swift equipped with the sophisticated detecting instruments. Furthermore, the debating issues on origins of GRBs (galactic or cosmological location) and the (isotropic or anisotropic distributions) of GRBs at early discovery of GRBs were confirmed in swift era.

Fire ball as the standard model developed during the swift era to explain the emission mechanisms of gamma-ray burst and its afterglows (from X-ray to radio band). However , the features of temporal and spectral indices x-ray afterglow were not yet clear as far as review of related literature concerned . So to solve this problem comprehensive methodology of qualitative and quantitative research approach and procedures are implemented to fill the knowledge gaps and to explain unclear issues mentioned in section 1.5 as well.

3.2 Research designs

3.2.1 Fire ball Models

As mentioned in section (2.2), the standard fireball model proposed to explain afterglow gamma-ray bursts. In standard fireball model, the behavior of X-ray light curves assumed to be characterize d by a single power law and broken power law decay model where flux fading time defined by :

$$f_\nu(t) \propto t^{-\alpha} \tag{3.1}$$

where $f_\nu$the flux decay with time and α is the temporal index/decay slope and subscript by numbers α = 1, 2, 3,and 4 for early steep decay slope, shallow or plateau decay slope, normal decay slope and late steep decay slope respectively ,

that were captured by the swift/XRT. This is the model that relates both temporal (α) and spectral (β) indices in standard fireball model as:

$$\alpha = 2 + \beta \tag{3.2}$$

is called the closure relation , where both β and α have no units.

3.2.2 spectral models

Several spectral functions models are available for use with gtlike.The power-law model is the simplest model that can be used to describe a GRB spectrum . This model consists of two parameters: the low-energy photon index α and normalization A. With these two parameters, the power-law model can fit the spectra of most GRBs if they are applicable to such a burst. This model is suitable when the signal-to-noise ratio of the fitting spectrum is very low and in the case when the signal is weak and if the break energy cannot be determined due to the break energy of the broken power-law spectrum lying outside the energy band of such a detector. The power-law spectral model for point source is defined by the equation below:[10]

3.2.3 Power law (PL)

$$\frac{dN}{dE} = N_o(E/E_o)^{-\gamma} \tag{3.3}$$

where the parameters in the XML definition have the following mappings:
Prefactor = N_o
Index = γ
Scale =E_o
and the units are $cm^{-2}\ s^{-2}\ MeV^{-2}$.

3.2.4 Numerical models: R-squared (R^2) , covariance and correlation coefficients

R^2 - R-squared - is the "percent of variance explained " by the model. In the same token, it is the fraction by which the variance of the error is less than variance. The values of R^2 ranges from 0 to 1 and typically expressed in percentage , and defined by the equation :

$$R^2 = \frac{SSR}{SST} = \frac{\sum(\hat{y}_i - \bar{y})^2}{\sum(y_i - \bar{y})^2} \tag{3.4}$$

where SSR- is the sum of square regression or the sum of square residuals.
SST -is the total sum square /sum square total.
$\hat{y}$ -is the prediction or points on the fitting line.
$\bar{y}$-mean of all the values.
y_i- is the actual values / points.
R- squared also defined as,

$$R^2 = 1 - \frac{\sum(\hat{y}_i - y_i)^2}{\sum(y_i - \bar{y}_i)^2} \tag{3.5}$$

The characteristic of light curves of gamma-ray afterglows determined by dispersion of variables (numbers of bursts versus time in space).How far the data spread or distributed around the mean / average values explained by correlation and covariance . The covariance of two dimensional data defined as :

$$cov(x, y) = \frac{1}{n-1} \sum_{i=1}^{n} (x_i - \bar{x})(y_i - \bar{y}) \tag{3.6}$$

Similarly , correlation coefficient of the same data given by :

$$r_{xy} = \frac{1}{n-1} \sum_{i=1}^{n} \frac{(x_i - \bar{x})}{sd(x)} \frac{(y_i - \bar{y})}{sd(y)} \tag{3.7}$$

If covaiance C (x, y) of two dimensional data were known , we use the equation:

$$r_{xy} = \frac{cov(xy)}{\sqrt{v(x)v(y)}} \tag{3.8}$$

, where cov (x , y) is covariance , sd(x) and sd(y) are standard divaition of x-data and y-data and they are square root of variance v(x) and v(y) respectively .The values of covariance of the data lies in the range of $-\infty$ and $+\infty$, where as the values of correlation coefficient r_{xy} limited b/n range -1.00 and +1.00 . The results of data analysis : C (x, y) and r_{xy} presented in table r_{xy} is correlation coefficient of x-data and y-data . In our case, x-data and y-data represent time (sec) and flux in $(erg/cm^{-2}s^{-1})$ respectively .

3.3 Type of data and its source

For our work , we used the existing secondary data type detected by Swift-XRT (evans et.al Online repository) over longer periods. In our sample , both the classes of gamma-ray bursts (short and long GRBs) are selected equally.

Table 3.1: Represents swift / xrt data sampled for long and short grb

Class of GRBs	LC with Break 1	LC with Break 2	LC with Break 3	Total
Short GRB	2	3	5	10
Long GRB	3	2	5	10
Total	5	5	10	20

3.4 Data sampling technique and size

Three Criterion were designed to select the required sample. i.e types of gamma-ray , the number of light curve breaks and well defined red shifts are used to select the desired sampled data. Based on mentioned criterion , twenty (20) GRBs afterglows are selected using simple random probability sampling method. The sampled GRBs afterglow data tabulated in table below.

3.5 Validity and reliability of data

As mentioned in section 3.3, examine the data then to get the information about object under taken , we already decided to follow both quantitative and qualitative approaches , standard models and tools were proposed to use in analyzing the data collected so as to achieve the desired objectives and answers for the statements of problems mentioned in section 1.5. This might be keep the validity and reliability of our work.

3.6 Data processing and analyzing

3.6.1 Data processing

As mentioned in section 3.3 above , twenty gamma -ray bursts (long and short) were collected as a sample to analyze. To extract relevant information and conclusions that support the final judgment , the sampled GRBs data were cleaned by avoiding duplicated , incorrect , and missing data .

3.6.2 Data analyzing

We analyze our sampled swift / xrt data to calculate the fitting parameters (temporal indices , amplitudes and covariance etc) , furthermore to observe and test how these parameters determine the features of light curves of x-ray afterglows . using

power law model and applying python 3 programming language , the plot of flux (F) against time (t) of sampled x-ray data has been shown respectively for long and short GRBs in fig.....and....fig below . The results of Calculated fitting parameters are also tabulated in table (a) and (b) section 4.1. using python 3 programming

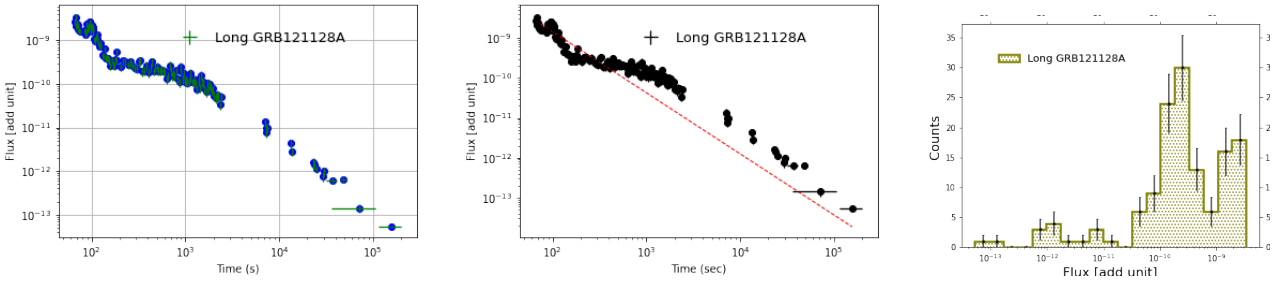

(a) **(b)** **(c)**

Figure 3.1: x-ray afterglow Light curve (a) , x-ray light curve fitting - red line (b) , and histogram of photons counts versus x-ray flux (c) of long GRB121128A .

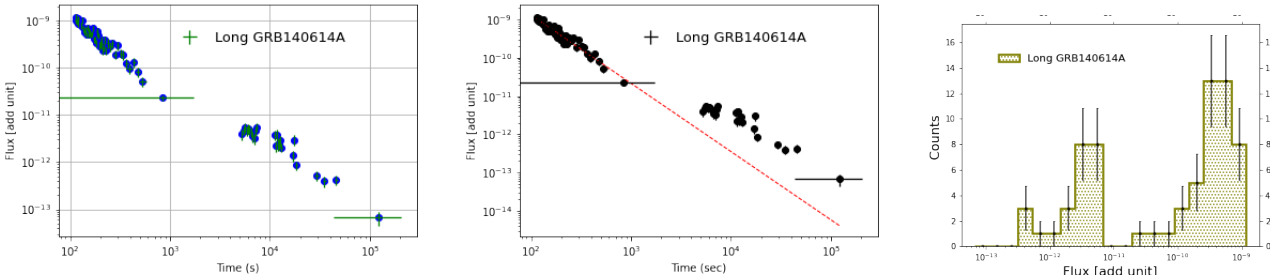

(a) **(b)** **(c)**

Figure 3.2: x-ray afterglow Light curve (a) , x-ray light curve fitting - red line (b) , and histogram of photons counts versus x-ray flux (c) of long GRB140614A .

language the fitting of five short GRBs have been performed and shown in figures below.

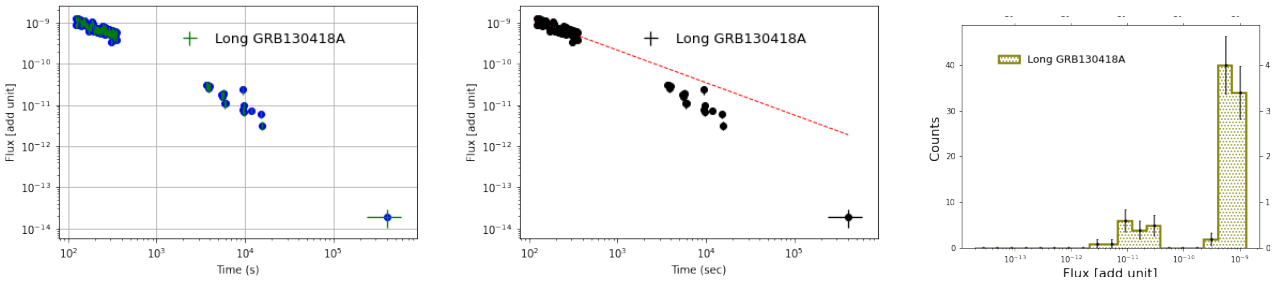

(a) **(b)** **(c)**

Figure 3.3: x-ray afterglow Light curve (a) , x-ray light curve fitting - red line (b) , and histogram of photons counts versus x-ray flux (c) of long GRB130418A .

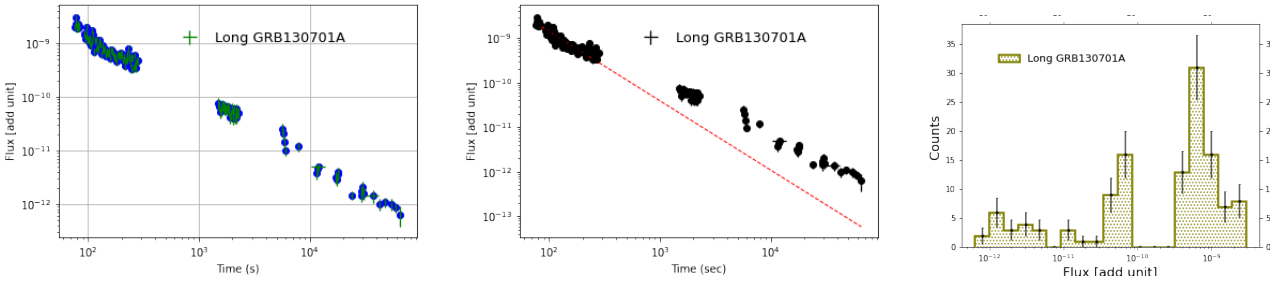

(a) **(b)** **(c)**

Figure 3.4: x-ray afterglow Light curve (a) , x-ray light curve fitting - red line (b) , and histogram of photons counts versus x-ray flux (c) of long GRB130701A .

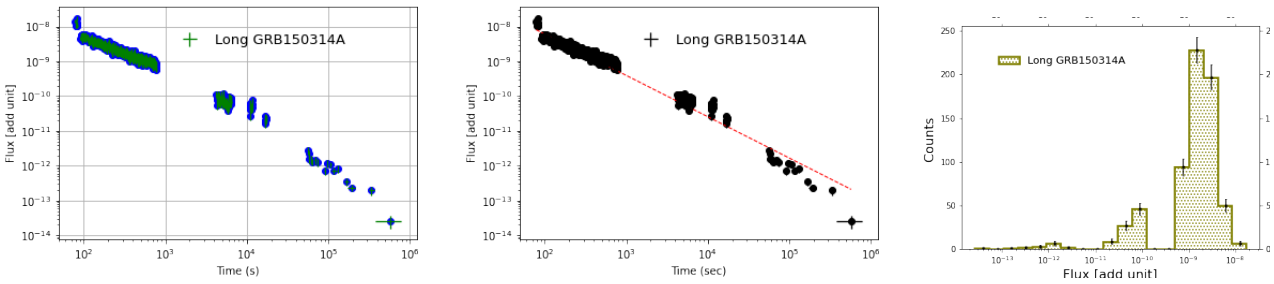

(a) **(b)** **(c)**

Figure 3.5: x-ray afterglow Light curve (a) , x-ray light curve fitting - red line (b) , and histogram of photons counts versus x-ray flux (c) of long GRB150314A .

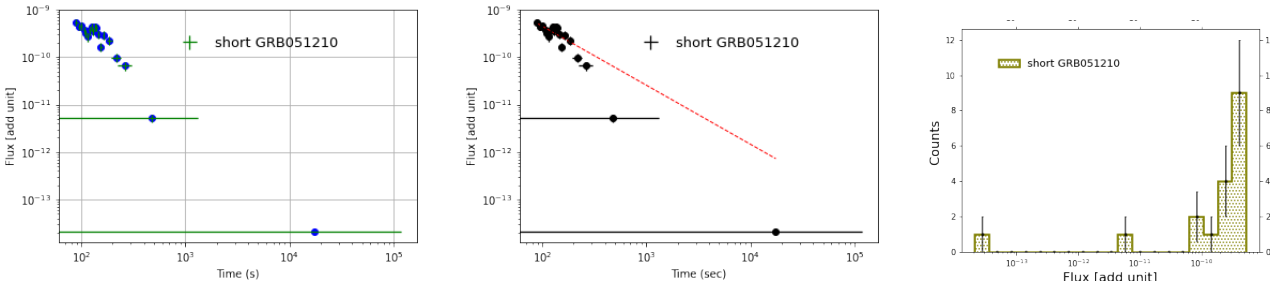

(a) **(b)** **(c)**

Figure 3.6: x-ray afterglow Light curve (a) , x-ray light curve fitting - red line (b) , and histogram of photons counts versus x-ray flux (c) of short GRB051210 .

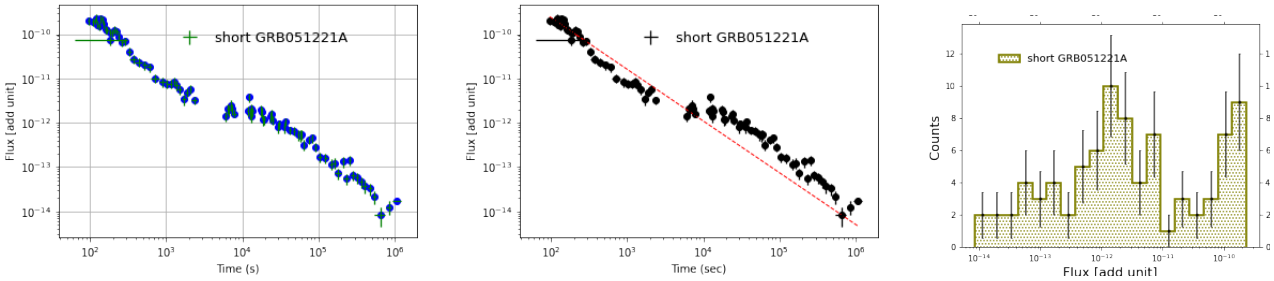

(a) **(b)** **(c)**

Figure 3.7: x-ray afterglow Light curve (a) , x-ray light curve fitting - red line (b) , and histogram of photons counts versus x-ray flux (c) of short GRB 051221A.

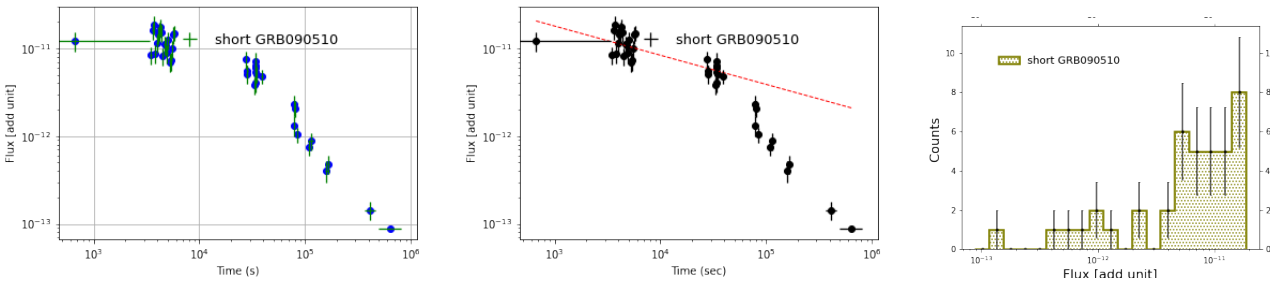

(a) **(b)** **(c)**

Figure 3.8: x-ray afterglow Light curve (a) , x-ray light curve fitting - red line (b) , and histogram of photons counts versus x-ray flux (c) of short GRB090510.

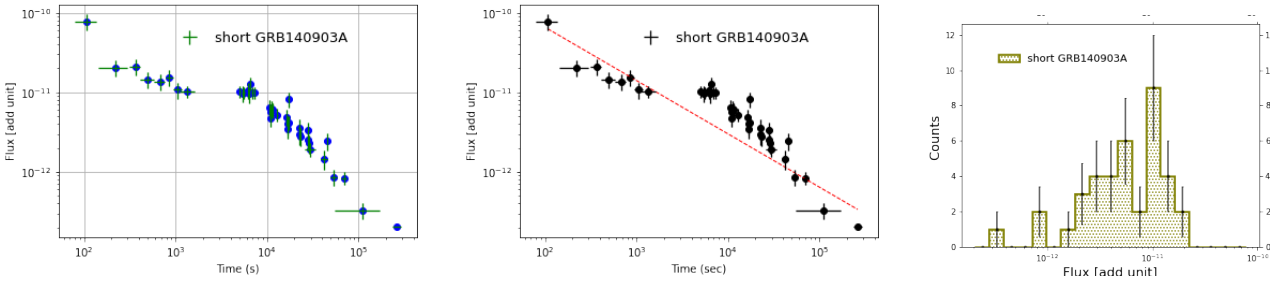

(a) **(b)** **(c)**

Figure 3.9: x-ray afterglow Light curve (a) , x-ray light curve fitting - red line (b) , and histogram of photons counts versus x-ray flux (c) of short GRB140903A.

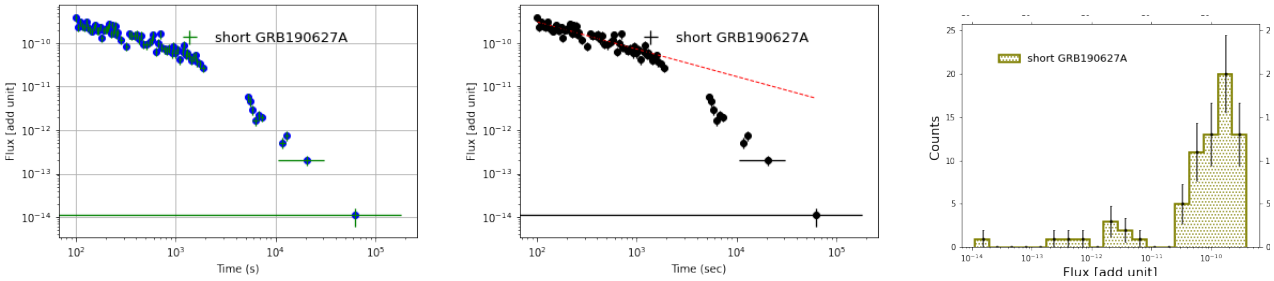

(a) **(b)** **(c)**

Figure 3.10: x-ray afterglow Light curve (a) , x-ray light curve fitting - red line (b) , and histogram of photons counts versus x-ray flux (c) of short GRB190627A.

CHAPTER 4

Result and discussion

Introduction

In this chapter, the results of swift / xrt data analysis (fitting parameters : temporal indices (slopes) , amplitudes (intercepts) , R-squared (R^2) , covariance and correlation coefficients etc) are summerized below in tables. Furthermore , the features of all fitting parameters would be interprated so as to confirm the consistency of the results of each x-ray afterglows with the proposed theories or models. Finally , the results are justified or disproved depending on the objectives of the thesis as well. As mentioned in section 2.4 above , early x-ray afterglow light curves composed of several components in which the canonical shape has four power law segments defined by : ($F_\nu \propto \nu^{-\beta} t^{-\alpha}$) , and were identified as :

• A fast intial decay : ($3 < \alpha_1 < 5$)

• A very shallow decay : ($0.5 < \alpha_2 < 1$)

• Intermediate (normal decay): ($1.0 < \alpha_3 < 1.5$)

• Late step decay with decaying index (α_4): and α_4 closer to 2 and was identified in pre - swift era. However , not all observed GRBs afterglow have all these 4 behviors /components. Here , we treat our resuts in relation to these bench marks.

4.1 Results of data analysis .

The sampled GRBs afterglow data that has been taken from swift / xrt light curves repository were analyzed for 5 long and 4 short GRBs with known red shift and T_{90} using python 3 programming language . The results of fitting parameters: temporal indices and amplitudes , covariance cov (x, y) , R^2 and correlation cofficients are respectively summerized in tables 4.1 and 4.2 , where as the dispersion parameters : variances σ^2 and standard divations σ were also summerized in table 4.3 below.

Table 4.1: Represents the resuts of calculated temporal indices σ and amplitudes (A) for sampled data has taken from swift / xrt data center

GRB name	class	$T_{90} > 2sec$	z	$Lc_{breakNo}$	α	A $\times 10^{-8}$
GRB140614A	long	233.90	4.23	2	$1.78^{+0.09}_{-0.09}$	$(4.81^{+2.27}_{-2.27})$
GRB130701A	long	4.38	1.16	1	$1.55^{+0.64}_{-0.64}$	$(1.87^{+0.55}_{-0.55})$
GRB121128A	long	23.30	2.20	2	$1.53^{+0.09}_{-0.09}$	$(1.69^{+0.73}_{-0.73})$
GRB150314A	long	14.79	1.76	1	$1.19^{+0.03}_{-0.03}$	$(1.43^{+0.18}_{-0.18})$
GRB051221A	short	1.40	0.55	2	$1.17^{+0.07}_{-0.07}$	$(5.10^{+0.17}_{-0.17})$
GRB130418A	long	>300	1.22	1	$0.78^{+0.05}_{-0.05}$	$(0.01^{+0.01}_{-0.01})$
GRB140903A	short	0.30	0.35	1	$0.67^{+0.06}_{-0.06}$	$(0.15^{+0.05}_{-0.05})$
GRB190627A	short	1.60	1.94	1	$0.63^{+0.04}_{-0.04}$	$(0.55^{+0.12}_{-0.12})$
GRB090510	short	0.30	0.90	1	$0.33^{+0.05}_{-0.05}$	$(0.02^{+0.01}_{-0.01})$

Table 4.2: Represents the .... of x-ray afterglow light curves

GRB name	Z	$\sigma_t^2 \times 10^{-3}$	σ_f^2	$\sigma_t \times 10^{-2}$	$\sigma_f \times^{-7}$
LGRB121128A	2.20	9.32	$53.6x10^{-14}$	9.65	7.320
LGRB140614A	4.23	8.79	$0.05x10^{-14}$	9.37	22.30
sGRB051221A	0,55	4.74	$0.03x10^{-14}$	6.8	17.40
LGRB130701A	1,16	4.11	$0.31x10^{-14}$	6.41	5.54
sGRB140903A	0.35	3.98	$2.50x10^{-19}$	6.30	0.005
sGRB090510	0.90	2.41	$5.57x10^{-21}$	4.90	0.001
LGRB130418A	1.22	2.40	$0.015x10^{-14}$	4.89	126.00
sGRB190627A	1.94	1.65	$1.42x10^{-18}$	4.06	0.119
LGRB150314A	1.76	0.67	$3.36x10^{-14}$	2.59	0.180

4.2 Discussion

In this section , we discussed on the features and messages of the parameters that resulted from curve fitting of our sampled swift /xrt data , there by interprating the results to observe the consistancy / inconsistancy occurs between depedent and indepedent variables . To interprate and justify the observed results of various parameters with the proposed models and existing theory , we discussed the features of parameters based on the results obtained from data analysis.

4.2.1 Interpreting parameters : Temporal indices / slopes

From the table 4.1 above , the temporal indices of all afterglow GRBs are consistent with the theoretical or proposed values of canonical x-ray afterglow light curves

GRB name	$T_{90}(s)$	Z	Lc_{breaks}	cov(t,f) x 10^{-8}	R^2	correlation r_{tf}
LGRB140614A	233.9	4.23	2	20.9	0.95	1.00
LGRB121128A	23.30	2.20	2	7.06	0.86	0.99
LGRB130418A	>300	1.22	1	6.18	0.91	0.99
LGRB130701A	4.38	1.16	1	3.56	0.93	1.00
LGRB150314A	14.79	1.76	1	0.47	0.83	0.99
sGRB051221A	1.40	0.55	2	0.12	0.95	1.00
sGRB190627A	1.60	1.94	1	0.05	0.87	0.99
sGRB090510	0.30	0.90	1	0.04	0.65	0.99
sGRB140903A	0.30	0.35	1	0.03	0.81	0.98

Table 4.3: Represents the covariance , R-squared , and correlation of x-data and y-data of x-ray afterglow light curves

, except (GRB 090510) with temporal index of $0.33^{+0.05}_{-0.05}$. Discussing in more detailed , the results of analysis in tables above , temporal indices of three GRBs : LGRB121128A , LGRB150314A and sGRB051221A with their respective errors are $1.53^{+0.09}_{-0.09}$, $1.19^{+0.03}_{-0.03}$ and $1.17^{+0.07}_{-0.07}$. when these results compared with the canonical power law segments , nearly closer to the values of normal decay phase ($1 < \alpha_3 < 1.5$) , and this scenario arises when the Lorentz factor Γ fall in forward shock model , and central engine / sources inactive.

Three GRBs : LGRB130418A , sGRB140903A and sGRB190627A each with one light curve break have respectively temporal indices of : $0.79^{+0.05}_{-0.05}$, $0.67^{+0.06}_{-0.06}$ and $0.63^{+0.04}_{-0.04}$. This results characterizing them as a very shallow / plateau decay phases of canonical x-ray afterglow since their values are consistent with the ($0.5 < \alpha_2 < 1$) and happend due to energy injected to a decelerated external shock.
From the table 4.1 above, two LGRBs : LGRB130701A and LGRB140614A each has temporal indices with errors $1.56^{+0.06}_{-0.06}$ and $1.78^{+0.09}_{-0.09}$ respectively . The value of temporal indices of each GRB nearly closer to 2 , characterizing them as the late steep decay phase of canonical x-ray afterglow that resulted from collimated ejecta when $\Gamma > \theta^{-1}$ compared to opening angle θ .Ingeneral, 88.8% (8/9) of the sampled GRBs afterglow x-ray consistent with canonical phase of x-ray afterglow.

4.2.2 Interpreting parameters : Amplitudes / intercepts

Amplitude -is one of the fitting parameter that characterizing the light curves of x- ray afterglow and equivalent to its intensity / brightness . LGRB121128A , LGRB150314A and sGRB051221A respectively $(1.69^{+}_{-}0.73) \times 10^{-8}$, $(1.43^{+0.18}_{-0.18}) \times 10^{-8}$, and $(5.1^{+0.17}_{-0.17}) \times 10^{-8}$

4.2.3 Interpreting :R^2 , cov (x,y) and correlation coefficients r_{xy}

using equations 3.4 and 3.5 , R-squared R^2 values of the data is calculated , and the results presented in table 4.3 . In the sample 6 GRBs afterglow (66.67%) have R-squared (R^2) values between 85% to 100% that nearest to 1 , indicating that the actual observed points are closer to points on prediction / fitting line , we call this best fitting line , which confirms that the variation / movement of dependent variable (afterglow x-ray flux) completely explained by independent variable (the time parameter). However , 33.3% of sampled GRBs afterglow have R^2 values less than or equal to 70% signalling that there is no best fitting line , this is due to larger distances b/n observed points and points on regression / fitting line.

Similarly , the results of data analysis (table 4.3) also suggests that , the directional relationship of two dimensional data (x and y-data) is negative , that agreed with the fact that , x-ray flux decaying / fading with time as the time increases. However , curve fitting show decaying rate differ for different GRB afterglow due to central engine activity and inhomogenity of the external medium (see fig 3.1 to fig 3.7). Furthermore , the correlation coefficients r_{xy} of the sampled data range from -0.98 to -1.00 that indicatinging that there is a strong negative relationship b/n dependent and independent variables.This is to mean that , the x-ray flux decying , as the time increases .

4.2.4 Interpreting : Histogam and error bars

CHAPTER 5

Conclusion

In section 3.5.2 , the plots of flux against time (light curves) of 10 GRBs are shown in fig 3 and fig 4 respectively. The light curves of each sampled GRBs were all decaying with time. However , due to activity of central engines (progenitors) and interaction of ejecta with circumbrust medium , some light curves of x-ray were decaying rapidly while the others slow.This is the common behavior of x-ray afterglows .

Bibliography

[1] Piran, Tsvi The physics of gamma-ray bursts journal , Reviews of Modern Physics (76),4 , 1145 ,2005

[2] Gomboc, Andreja Unveiling the secrets of gamma ray bursts , *Contemporary Physics , (53),(4) 339–355 , 2012* Taylor & Francis

[3] Gehrels, Neil and Ramirez-Ruiz, E and Fox, Derek B Gamma-ray bursts in the Swift era , *arXiv preprint arXiv:0909.1531 , 2009*

[4] Palmerio, Jesse Gamma-ray burst production efficiency from stars: *constraints from population models and host galaxies , 2018, , Sorbonne universit*

[5] Zhang, Binbin A Multi-wavelength study on gamma-ray bursts and their afterglows ,2011

[6] Dereli, Hüsne Study of a Population of Gamma-ray Bursts with Low-Luminosity Afterglows , *arXiv preprint arXiv:1503.04580 , 2015*

[7] Hu, You-Dong Multi-wavelength study of GRBs detected by Fermi and Swift , 2021 , Universidad de Granada

[8] Margutti, Raffaella and Zaninoni, E and Bernardini, MG and Chincarini, G and Pasotti, F and Guidorzi, C and Angelini, Lorella and Burrows, DN and Capalbi, M and Evans, Phil A and others The prompt-afterglow connection in gamma-ray bursts: a comprehensive statistical analysis of Swift X-ray light curves , *Monthly Notices of the Royal Astronomical Society , (428), (1) , 729–742 , 2013 , Oxford University Press*

[9] Gupta, Rahul and Oates, SR and Pandey, SB and Castro-Tirado, AJ and Joshi, Jagdish C and Hu, YD and Valeev, AF and Zhang, BB and Zhang, Z and Kumar, Amit and others GRB 140102A: insight into prompt spectral evolution and early optical afterglow emission , *Monthly Notices of the Royal Astronomical Society ,(505),(3), 4086–4105 2021, Oxford University Press*

[10] Moneer, Eman Spectral Analysis of GRBs Observed by Swift and Fermi Satellites , 2019 , University of Leicester

[11] IceCube Collaboration and Fermi-LAT and MAGIC and AGILE and ASAS-SN and HAWC and HESS and INTEGRAL and Kanata and Kiso and others Multimessenger observations of a flaring blazar coincident with high-energy neutrino IceCube-170922A , *Science (361) ,(6398), eaat1378 , 2018*

[12] Sari, Re'em and Piran, Tsvi Variability in GRBs-A Clue , *Arxiv preprint astro-ph/9701002 , 1997*

[13] Knust, Fabian Applying the Fireball Model to Short Gamma-Ray Burst Afterglows: Methods, Jet Opening Angles and Plateau Phases , 2017 ,Technische Universität München

[14] Dainotti, MG and Del Vecchio, Roberta Gamma Ray Burst afterglow and prompt-afterglow relations: *An overview New Astronomy Reviews ,(77) 23–61 ,2017*

[15] Vedrenne, Gilbert and Atteia, Jean-Luc Gamma-ray bursts: The brightest explosions in the universe , 2009, sprigerscience& business media

[16] Turpin, D and Heussaff, V and Dezalay, J-P and Atteia, JL and Klotz, A and Dornic, D Connecting Prompt and Afterglow GRB emission I. Investigating the impact of optical selection effects in the Epi-Eiso plane , *arXiv preprint arXiv:1503.02760 2015*

[17] Piran, Tsvi Gamma-ray bursts and the fireball model , Physics Reports, (314) (6) 575–667 , 1999

[18] Kumar, Pawan and Zhang, Bing The physics of gamma-ray bursts & relativistic jets , *Physics Reports , (561) 177–109, 2015*

[19] Sokolov, VV and Bisnovatyi-Kogan, GS and Kurt, VG and Gnedin, Yu N and Baryshev, Yu V Observational constraints on the angular and spectral distributions of photons in gamma-ray burst source *Astronomy reports (50), (8) 612–625, 2006*,

[20] Piran, Tsvi Magnetic Fields in Gamma-Ray Bursts: A Short Overview , Piran, Tsvi , *AIP Conference Proceedings , (784),(1) 164–174 , 2005*

[21] Lipunov, Vladimir and Simakov, Sergey and Gorbovskoy, Evgeny and Vlasenko, Daniil Smooth optical self-similar emission of gamma-ray bursts , *The Astrophysical Journal , (845),(1), (52) 2017*

[22] Pe'Er, Asaf Physics of gamma-ray bursts prompt emission , Advances in Astronomy , (2015) , 2015

[23] Ukwatta, Tilan Spectral lags and variability of Gamma-ray Bursts in the Swift era , The George Washington University , 2011

[24] Podsiadlowski, Philipp and Oswalt, TD and Barstow, MA Supernovae and gamma ray bursts ,*Planets, Stars and Stellar Systems. Volume 4: Stellar Structure and Evolution ,(4),(693), 2013*

[25] Dar, Arnon and De Rújula, Alvaro Towards a complete theory of gamma-ray bursts , Physics Reports ,(405), (4),(203–278),2004

[26] Fargion, Daniele and Oliva, Pietro Solving the missing GRB neutrino and GRB , Nuclear and particle physics proceeding (297),(249–258), 2018

[27] Mazzali, Paolo A and Kawabata, Koji S and Maeda, Keiichi and Nomoto, Ken'ichi and Filippenko, Alexei V and Ramirez-Ruiz, Enrico and Benetti, Stefano and Pian, Elena and Deng, Jinsong and Tominaga, Nozomu and others An asymmetric energetic type Ic supernova viewed off-axis, and a link to gamma ray bursts ,*Science , (308) , (5726) , (1284–1287) 2005 , American Association for the Advancement of Science*

[28] Levan, Andrew J Gamma-ray bursts and their environments , 2005 , University of Leicester United Kingdom

[29] Salaris, Maurizio and Cassisi, Santi Evolution of stars and stellar populations , 2005 , John Wiley & Sons

[30] Meszaros, Peter Gamma-ray bursts , *Reports on Progress in Physics ,(69), (98),(2259) 2006 , IOP Publishing*

[31] Yi, Shuang-Xi and Xie, Wei and Ma, Shuai-Bing and Lei, Wei-Hua and Du, Mei Constraining properties of GRB central engines with X-ray flares , Monthly Notices of the Royal Astronomical Society ,(507), (1),(1047–1054) , 2021 , Oxford University Press

[32] Willingale, R and O'brien, PT and Osborne, JP and Godet, O and Page, KL and Goad, MR and Burrows, DN and Zhang, B and Rol, E and Gehrels, N and others Testing the standard fireball model of gamma-ray bursts using late X-ray afterglows measured by Swift ,*The Astrophysical (662),(2),(1093), 2007*

[33] Zhang, Bing A burst of new ideas *Nature ,444 , 7122 , 1010–1011 , 2006 , Nature Publishing Group*

[34] Piran, Tsvi Gamma-ray bursts–a puzzle being resolved , *Physics Reports , 333 , 529–553 , 2000 , Elsevier*

[35] Del Vecchio, Roberta and Dainotti, Maria Giovanna and Ostrowski, Michał Study of GRB light-curve decay indices in the afterglow phase , *The Astrophysical Journal (828), (1) ,(36), 2016*

[36] HESS collaboration and Abdalla, H and Aharonian, F and Ait Benkhali, F and Angüner, EO and Arcaro, C and Armand, C and Armstrong, T and Ashkar, H and Backes, M and others Revealing x-ray and gamma ray temporal and spectral similarities in the GRB 190829A afterglow , Science , (372) , 6546 ,(1081–1085), 2021 , American Association for the Advancement of Science

[37] Fan, YZ and Wei, DM Late internal-shock model for bright X-ray flares in gamma-ray burst afterglows and GRB 011121 , Fan, YZ and Wei, DM , *Monthly Notices of the Royal Astronomical Society: Letters ,(364),(1),(L42–L46),2005*

[38] Fan, Yizhong and Piran, Tsvi Gamma-ray burst efficiency and possible physical processes shaping the early afterglow , *Monthly Notices of the Royal Astronomical Society , (369),(1),(197–206), 2006 , The Royal Astronomical Society*

[39] Mangano, Vanessa and La Parola, Valentina and Cusumano, Giancarlo and Mineo, Teresa and Malesani, Daniele and Dyks, Jaroslaw and Campana, Sergio and Capalbi, Milvia and Chincarini, Guido and Giommi, Paolo and others . Swift XRT observations of the afterglow of XRF 050416A ,*The Astrophysical Journal , (654),(1),(403),(2007), IOP Publishing*

[40] Ramirez-Ruiz, Enrico and Dray, Lynnette M and Madau, Piero and Tout, Christopher A Winds from massive stars: implications for the afterglows of γ-ray bursts , Monthly Notices of the Royal Astronomical Society , (327),(3), (829–840), (2001) Blackwell Science Ltd Oxford, UK

[41] Lee, Chang-Hwan and Brown, Gerald E On the theory of gamma ray bursts and hypernovae: The black hole soft X-ray transient sources , International Journal of Modern Physics A , (18), 04), (527–576), 2003 , World Scientific

[42] Rees, Martin J and Mészáros, Peter Dissipative photosphere models of gamma-ray bursts and X-ray flashes ,*The Astrophysical Journal ,(628), (2), (847), 2005*,

[43] Granot, Jonathan and Sari, Re'em The shape of spectral breaks in gamma-ray burst afterglows , The Astrophysical Journal , (568), (2), (820), 2002,

[44] Ghisellini, G and Ghirlanda, G and Nava, L and Firmani, C "Late Prompt" emission in gamma-ray bursts? , The Astrophysical Journal ,(658),(2),(L75), 2007 ,IOP Publishing

[45] Wijers, RAMJ and Galama, TJ Physical parameters of GRB 970508 and GRB 971214 from their afterglow synchrotron emission ,The Astrophysical Journal , (523), (1), (177), 1999 ,IOP Publishing

[46] McClintock, JE and Remillard, RA and Lewin, WHG and van der Klis, Michiel Compact stellar X-ray sources ,(2006), Cambridge Univ. Press Cambridge

[47] Selsing, Jonatan Illuminating the dark: with cosmic explosions and their afterglows , Ph. D. Thesis , 2018

[48] Harrison, FA and Bloom, JS and Frail, Dale A and Sari, R and Kulkarni, Shrinivas R and Djorgovski, SG and Axelrod, Tim and Mould, Jeremy and Schmidt, Brian P and Wieringa, Mark H and others Optical and Radio Observations of the Afterglow from GRB 990510: Evidence for a Jet , The Astrophysical Journal , (523) ,(92), (L121), 1999

[49] Wijers, RAMJ and Galama, TJ Physical parameters of GRB 970508 and GRB 971214 from their afterglow synchrotron emission , *The Astrophysical Journal (523),(1),(177),(1999)*

[50] Costa, E etal and Frontera, F and Heise, J and Feroci, M al and Fiore, F and Cinti, MN and Dal Fiume, D and Nicastro, L and Orlandini, M and Palazzi, E and others Discovery of an X-ray afterglow associated with the γ-ray burst of 28 February 1997 , Nature, (387), (6635) ,(783–785),1997

[51] Zhang, Bing and Mészáros, Peter High- energy spectral components in gamma-ray burst afterglows , The Astrophysical Journal , (559)(1), (110), 2001

[52] Vergani, Susanna D Studies on the gamma-ray burst phenomenon and on its use to probe the high redshift universe ,2009

DECLARATION

ADDIS ABABA UNIVERSITY
COLLEGE OF NATURAL AND COMPUTATIONAL SCIENCES
DEPARTMENT OF PHYSICS

MSc Thesis

Light Curve Characterstics of Gamma-Ray Burst

Name of Candidate: Temam Beyan Tuki

I the under signed declare that the thesis is my original work and no part of it can be claimed as an intellectual property of anybody else except me and my advisors.

Signature: _____